National Technical University of Athens
School of Electrical and Computer Engineering
Division of Power Electronics

Clearing of Reserve and Energy Markets with Multiple Reserve Products

Diploma Thesis

Ioannis Verrios

Supervisor: Anthony Papavasiliou
Professor, NTUA

Athens, October 2025

National Technical University of Athens
School of Electrical and Computer Engineering
Division of Power Electronics

Clearing of Reserve and Energy Markets with Multiple Reserve Products

Diploma Thesis

Ioannis Verrios

Supervisor: Anthony Papavasiliou
Professor, NTUA

Approved by the three-member scientific committee on 30 October 2025:

Papavasiliou Antonios Professor, NTUA	Georgilakis Pavlos Professor, NTUA	Dimeas Aris Assistant Professor, NTUA

Athens, October 2025

(Signature)

. . . .

Ioannis Verrios
Graduate of School of Electrical and Computer Engineering, National Technical University of Athens

Περίληψη

Η μεγάλη ενσωμάτωση ανανεώσιμων πηγών ενέργειας και το διαρκώς αυξανόμενο απρόβλεπτο φορτίο στα συστήματα ηλεκτρικής ενέργειας, καθιστούν σημαντικό τον ρόλο των εφεδρειών στις αγορές εκκαθάρισης ενέργειας και εφεδρειών. Αυτή η διπλωματική εργασία διερευνά εναλλακτικούς μηχανισμούς εκκαθάρισης αγοράς και συγκρίνει μοντέλα συν-βελτιστοποίησης (co-optimization) και ακολουθιακών (sequential) σχεδιασμών.

Αναλύθηκαν τρεις μέθοδοι εκκαθάρισης: (α) ένα μοντέλο συν-βελτιστοποίησης ενέργειας και εφεδρειών, (β) ένα ακολουθιακό μοντέλο με ταυτόχρονη εκκαθάριση προϊόντων εφεδρείας και (γ) ένα ακολουθιακό μοντέλο με ξεχωριστή εκκαθάριση προϊόντων εφεδρείας. Διατυπώθηκαν τα μαθηματικά μοντέλα και για τις τρεις μεθόδους και υλοποιήθηκαν σε Julia και εφαρμόστηκαν στο σύστημα του Βελγίου.

Τα αποτελέσματα δείχνουν ότι η συν-βελτιστοποίηση είναι σταθερά αποδοτικότερη, μειώνοντας το συνολικό κόστος συστήματος και αξιοποιώντας καλύτερα τους πόρους, ενώ οι ακολουθιακές μέθοδοι εισάγουν αναποτελεσματικότητες λόγω της σταδιακής εκκαθάρισης της ενέργειας και των εφεδρειών. Αυτές οι αναποτελεσματικότητες γίνονται ιδιαίτερα εμφανείς σε συνθήκες έλλειψης ευέλικτων πόρων και συγκεκριμένα σε συνθήκες μείωσης της δυνατότητας παραγωγής από τις μονάδες αντλησιοταμίευσης.

Τα ευρήματα δείχνουν τα οικονομικά οφέλη από την υιοθέτηση της συν-βελτιστοποίησης στις ευρωπαϊκές αγορές ηλεκτρικής ενέργειας, όπου η ακολουθιακή εκκαθάριση παραμένει η κύρια πρακτική. Πέρα από τις αριθμητικές αναλύσεις, η εργασία προσφέρει ένα ευέλικτο υπολογιστικό πλαίσιο που μπορεί να προσαρμοστεί για να συμπεριλάβει περιορισμούς δικτύου, μεταβλητά προφίλ ανανεώσιμων πηγών ενέργειας ή ανταλλαγή δυναμικότητας εφεδρείας μεταξύ χωρών. Σε γενικές γραμμές, η ανάλυση παρέχει τόσο μεθοδολογικές γνώσεις όσο και στοιχεία σημαντικά για τη χάραξη πολιτικής υπέρ σχεδιασμών αγοράς που ενσωματώνουν την ενέργεια και τις εφεδρείες για τη βελτίωση της αποδοτικότητας και της αξιοπιστίας της λειτουργίας του συστήματος ηλεκτρικής ενέργειας.

Λέξεις Κλειδιά: Συν-βελτιστοποίηση, Ακολουθιακή εκκαθάριση, Αγορές ενέργειας, Αγορές εφεδρειών, Μαθηματική μοντελοποίηση, Συντονισμός ενέργειας και εφεδρειών, Λειτουργικό κόστος συστήματος, Υλοποίηση προγραμματισμού Julia, Ρόλος Αντλησιοταμιευτικών Υδροηλεκτρικών

Abstract

The large integration of renewable energy sources and growing unforeseen load into power systems increases the importance of effective coordination between energy and reserve markets. This thesis investigates alternative market clearing mechanisms, focusing on the comparison between co-optimization and sequential designs. A mathematical framework was developed to capture the interdependencies between energy and multiple reserve products, aFRR and mFRR, while accounting for technical constraints such as ramping limits, minimum up and down times, start-up costs and pumped-storage dynamics.

Three distinct clearing methods were analyzed: (i) a co-optimization model of energy and reserves, (ii) a sequential model with joint reserve allocation, and (iii) a sequential model with separate clearing of reserve types. The mathematical methodologies were formulated and implemented in Julia and applied to the Belgian system.

Results indicate that co-optimization consistently delivers more efficient outcomes by reducing total system costs and making better use of inflexible low-cost resources, while sequential methods introduce inefficiencies due to their staged handling of energy and reserves. These inefficiencies become particularly apparent under scarcity of flexible resources, specifically under conditions of reduced generation capability from Pumped-Storage Hydro units.

The findings reveal the financial benefits of adopting co-optimization in European electricity markets, where sequential clearing remains the main practice. Beyond numerical insights, the thesis offers a flexible computational framework that can be adapted to include network constraints, variable renewable energy profiles, or reserve capacity exchange between countries. In general, the analysis provides both methodological insights and evidence important for policy in favor of market designs that integrate energy and reserves to improve the efficiency and reliability of power system operation.

Keywords: Co-optimization, Sequential clearing, Energy markets, Reserve markets, Mathematical modeling, Energy and reserve coordination, System operation costs, Julia programming implementation, Pumped-Storage Hydro role

Acknowledgements

I express my gratitude to my supervisor, Professor Anthony Papavasiliou, and his research team for providing me with the opportunity to contribute to the important work they have developed in power systems research over the past years. I also extend my thanks to Dr. Daniel Ávila. From the moment this thesis topic was assigned to me, Daniel was by my side every week, always ready to answer my questions and guide me through every difficulty I encountered. His guidance and support were invaluable to the completion of this work.

Furthermore, I thank all my professors at the National Technical University of Athens (NTUA) for providing the essential knowledge and technical skills that formed the foundation for this thesis, as well as for my future engineering career.

Finally, I would like to thank my university friends, lifelong companions and family. They provided necessary guidance and strength to push forward during challenging moments, supporting me unconditionally on this journey.

Contents

List of Figures

Κεφάλαιο 1

Εκτενής Περίληψη

1.1 Εισαγωγή και Σκοπός της Εργασίας

Με αυτή τη διπλωματική εργασία, τρεις μηχανισμοί εκκαθάρισης στις αγορές ηλεκτρικής ενέργειας αναλύονται και συγκρίνονται ως προς την οικονομική τους αποδοτικότητα, η Συν-βελτιστοποίηση ενέργειας και εφεδρειών (Co-optimization) και η Ακολουθιακή Εκκαθάριση ενέργειας και εφεδρειών (Sequential Clearing), με Ξεχωριστή (Separate) και με Ταυτόχρονη (Joint) Εκκαθάριση Εφεδρειών.

Η ραγδαία αύξηση των απρόβλεπτων από την φύση τους Ανανεώσιμων Πηγών Ενέργειας (ΑΠΕ), καθώς και το διαρκώς αυξανόμενο φορτίο, καθιστούν αναγκαία αυτή τη σύγκριση, καθώς τα προιόντα εφεδρείας (όπως η αυτόματη εφεδρεία αποκατάστασης συχνότητας, aFRR, και η χειροκίνητη εφεδρεία αποκατάστασης συχνότητας, mFRR) έχουν αναλάβει κεντρικό ρόλο στην ασφάλεια και το λειτουργικό κόστος του συστήματος.

Ενώ η Συν-βελτιστοποίηση αναγνωρίζεται ως η πιο αποδοτική μέθοδος θεωρητικά αλλά και εμπειρικά από αγορές όπως οι ΗΠΑ, η ευρωπαϊκή αγορά παραμένει δεσμευμένη στο μοντέλο της Ακολουθιακής Εκκαθάρισης, η οποία καταλήγει σε δομικά σφάλματα.

Κεντρικός Στόχος της εργασίας λοιπόν, είναι η ποσοτικοποίηση αυτών των σφαλμάτων. Συγκεκριμένα, η μελέτη επικεντρώνεται σε δύο άξονες. Πρώτα στη συστηματική αξιολόγηση του συνολικού κόστους συστήματος που προκύπτει από τρία διαφορετικά μοντέλα: την συν-βελτιστοποίηση, την ακολουθιακή με κοινή εκκαθάριση εφεδρειών (Sequential Joint) και την ακολουθιακή με ξεχωριστή εκκαθάριση εφεδρειών (Sequential Separate - η τρέχουσα ευρωπαϊκή πρακτική). Έπειτα αναλύεται η κατανομή των πόρων, και ιδιαίτερα ο κρίσιμος ρόλος των ευέλικτων μονάδων, όπως τα Αντλησιοταμιευτικά Υδροηλεκτρικά (PSH).

1.2 Μεθοδολογία και Μοντελοποίηση

Και για τα τρία μοντέλα αναπτύχθηκαν οι λεπτομερείς μαθηματικές μεθοδολογίες βελτιστοποίησης, οι οποίες προσομοιώνουν την λειτουργία της αγοράς ηλεκτρικής ενέργειας και εφεδρειών. Ύστερα εφαρμόστηκαν στη γλώσσα προγραμματισμού Julia και επιλύθηκαν με τον βελτιστοποιητή Gurobi, δίνοντας τα απαραίτητα δεδομένα για την μετέπειτα ανάλυση.

1.2.1 Τα Τρία Μοντέλα Εκκαθάρισης

- **Μοντέλο Συν-βελτιστοποίησης (Co-optimization):** Ένα ενιαίο, ολοκληρωμένο μοντέλο που ελαχιστοποιεί το συνολικό κόστος συστήματος, προσδιορίζοντας ταυτόχρονα την παραγωγή ενέργειας και την κατανομή όλων των προϊόντων εφεδρείας (aFRR και mFRR). Η υπεροχή του έγκειται στην ικανότητά του να υπολογίζει με ακρίβεια το κόστος ευκαιρίας για κάθε μονάδα παραγωγής.

- **Ακολουθιακό Μοντέλο με Ταυτόχρονη & Ξεχωριστή Εκκαθάριση Εφεδρειών (Sequential Joint & Separate):** Τα μοντέλα ακολουθιακής εκκαθάρισης απαρτίζονται από τρία στάδια. Διαφέρουν μόνο στο δεύτερο στάδιο.

    1. Εκτίμηση Τιμής Ενέργειας (λ_t): Η τιμή της ενέργειας υπολογίζεται με τον βέλτιστο τρόπο, δηλαδή με το μοντέλο της συν-βελτιστοποίησης, οπότε μπορεί να θεωρηθεί ότι δεν εισάγει σφάλμα στο τελικό αποτέλεσμα. Η τιμή προκύπτει χρησιμοποιείται για τον υπολογισμό του κόστους ευκαιρίας στο επόμενο στάδιο.
    2. Εκκαθάριση Εφεδρειών: Γίνεται εκκαθάριση των δύο προϊόντων εφεδρείας aFRR και mFRR, είτε ταυτόχρονη (joint) είτε ξεχωριστή (separate), δεσμεύοντας την απαραίτητη ποσότητα.
    3. Τελική Εκκαθάριση Ενέργειας: Υπολογίζεται η τελική παραγωγή, με τις δεσμεύσεις εφεδρειών του προηγούμενου σταδίου να αποτελούν πλέον σταθερές στους περιορισμούς για την λειτουργία των μονάδων.

1.2.2 Εφαρμογή σε Πραγματικό Σενάριο (Case Study)

Το πραγματικό σενάριο που μελετήθηκε ήταν στο σύστημα του Βελγίου, λαμβάνοντας υπόψη τον εθνικό στόλο παραγωγής (πυρηνική βάση, θερμικές μονάδες, ΑΠΕ, Αντλησιοταμίευση) και τους τεχνικούς περιορισμούς των μονάδων (όρια ράμπας, ελάχιστος χρόνος λειτουργίας/παύσης και κόστη εκκίνησης). Για την εκτίμηση του ετήσιου κόστους, χρησιμοποιήθηκαν οκτώ αντιπροσωπευτικά σενάρια, δύο για κάθε εποχή: καθημερινή και ημέρα Σαββατοκύριακου.

1.3 Αποτελέσματα και Ανάλυση Αποδοτικότητας Μοντέλων

Τα αποτελέσματα των τριών μοντέλων επιβεβαιώνουν την οικονομική υπεροχή της συν-βελτιστοποίησης σε όλα τα εξεταζόμενα σενάρια. Αποκαλύπτεται έτσι το σημαντικό χρηματοοικονομικό βάρος που προκαλεί η ακολουθιακή προσέγγιση.

1.3.1 Ετήσιο Σφάλμα

Με την χρήση των αποτελεσμάτων για τις οκτώ αντιπροσωπευτικές μέρες, υπολογίζεται το ετήσιο κόστος παραγωγής ενέργειας για κάθε μοντέλο. Η ακολουθιακή εκκαθάριση αποδείχτηκε ότι εισάγει συστηματική σπατάλη πόρων σε σχέση με το βέλτιστο μοντέλο συν-βελτιστοποίησης.

Μοντέλο Εκκαθάρισης	**Ετήσιο Κόστος [€]**
Συν-βελτιστοποίηση	615.131.456
Ακολουθιακό με Ταυτόχρονη Εκκαθάριση Εφεδρείας	673.232.384
Ακολουθιακό με Ξεχωριστή Εκκαθάριση Εφεδρείας	673.235.144

Πίνακας 1.1: Ετήσιο Κόστος Παραγωγής Ηλεκτρικής Ενέργειας για τα τρία Μοντέλα

Τα αριθμητικά αποτελέσματα φαίνονται στον Πίνακα 1.1. Συγκρίνοντας τα δύο ακολουθιακά μοντέλα με την βέλτιστη συν-βελτιστοποίηση, εντοπίζονται σφάλματα της τάξης του 8,63%. Επιπλέον, το ακολουθιακό μοντέλο με ξεχωριστή εκκαθάριση εφεδρειών, το οποίο εφαρμόζεται και στην Ευρώπη, αποδείχθηκε η λιγότερο αποδοτική επιλογή, επιβαρύνοντας το σύστημα με επιπλέον 58.103.688 € ετησίως σε σχέση με την συν-βελτιστοποίηση.

Η αναποτελεσματικότητα των δύο ακολουθιακών σχεδιασμών, αποδίδεται κυρίως στο άκαμπτο, πολυσταδιακό τους σύστημα αποφάσεων.

Στο στάδιο εκκαθάρισης των εφεδρειών, οι δύο αυτές μέθοδοι αναγκάζονται να δεσμεύσουν ακριβές θερμικές μονάδες για να καλύψουν τα ζητούμενη εφεδρεία. Μόλις δεσμευτούν για εφεδρεία αυτές οι μονάδες, υποχρεούνται να λειτουργούν τουλάχιστον στο τεχνικό τους ελάχιστο κατά το τελικό στάδιο εκκαθάρισης ενέργειας, ακόμα κι αν υπάρχουν φθηνότερες διαθέσιμες πηγές (όπως αντλησιοταμίευση). Αντίθετα, το μοντέλο συν-βελτιστοποίησης αξιοποιεί πλήρως το λειτουργικό περιθώριο της αντλησιοταμίευσης για ενέργεια και εφεδρεία. Αυτή η αναγκαστική ακριβή παραγωγή είναι και ο κύριος λόγος που αυξάνει το συνολικό λειτουργικό κόστος του συστήματος.

1.3.2 Ανάλυση Ευαισθησίας Αντλησιοταμίευσης

Για να δοκιμαστεί η ανθεκτικότητα κάθε μοντέλου σε συνθήκες σπανιότητας ευέλικτων πόρων, πραγματοποιήθηκε ανάλυση ευαισθησίας μειώνοντας τη διαθέσιμη δυνατότητα παραγωγής ενέργειας από αντλησιοταμίευση (με πολλαπλασιαστές 1,0, 0,9 και 0,8). Τα αποτελέσματα έδειξαν ξεκάθαρη υπεροχή του μοντέλου συν-βελτιστοποίησης και σε αυτόν τον τομέα, καθώς όσο μειώνεται η δυνατότητα παραγωγής από αυτές τις μονάδες, το σφάλμα των ακολουθιακών μοντέλων κλιμακώνεται.

Επιπλέον, όταν ο πολλαπλασιαστής μειωθεί κάτω από το 0,8 (π.χ. γίνει 0.7), Τα ακολουθιακά μοντέλα καθίστανται μη επιλύσιμα.

Τα παραπάνω περαιτέρω ενισχύουν την υπεροχή της συν-βελτιστοποίησης στο να εκκαθαρίζει με τον βέλτιστο τρόπο κάθε φορά τις διαθέσιμες μονάδες και τονίζουν την δομική αδυναμία των ακολουθιακών στο να συμβαδίζουν.

1.4 Συμπεράσματα

Η παρούσα διπλωματική εργασία προσφέρει μια σαφή και μετρήσιμη τεκμηρίωση υπέρ της υιοθέτησης της συν-βελτιστοποίησης ενέργειας και εφεδρειών στις ευρωπαϊκές αγορές. Τα βασικότερα συμπεράσματα είναι:

- Από οικονομικής άποψης, η συν-βελτιστοποίηση είναι η μόνη μέθοδος που επιτυγχάνει τη βέλτιστη κατανομή πόρων, οδηγώντας σε μείωση του ετήσιου λειτουργικού κόστους του συστήματος (έως και 58.1 εκατ. € ετησίως για το Βέλγιο).

- Έπειτα, η σύγχρονη εκκαθάριση ενέργειας και εφεδρειών προσδίδει υψηλότερη ανθεκτικότητα απέναντι στη σπανιότητα ευέλικτων πόρων, όπως η αντλησιοταμίευση, και την αστάθεια των ΑΠΕ, σε αντίθεση με τα Διαδοχικά μοντέλα που καταρρέουν υπό συνθήκες πίεσης.

- Τέλος τα ευρήματα υποστηρίζουν τις ευρωπαϊκές ρυθμιστικές μεταρρυθμίσεις που βρίσκονται σε εξέλιξη, καθώς και την συνέχιση της έρευνας για την ενσωμάτωση τέτοιων μοντέλων στις αγορές.

Κλείνοντας, η μετάβαση από ένα ακολουθιακό μοντέλο σε ένα συν-βελτιστοποίησης στην Ευρώπη είναι αναγκαία για τη διασφάλιση της οικονομικής αποδοτικότητας, της αξιοπιστίας και της βέλτιστης αξιοποίησης των ευέλικτων πόρων σε ένα ηλεκτρικό σύστημα που εξαρτάται ολοένα και περισσότερο από τις Ανανεώσιμες Πηγές Ενέργειας.

Chapter 2

Introduction

2.1 Market Context

Since the introduction of electricity into modern societies, the use of reserves has consistently played a crucial role in bridging the gap created by unpredictable demands and unexpected system imbalances. At the beginning of modern electrification, reserves were mainly aimed at coping with demand uncertainty and occasional generator outages. However, recent decades with large-scale energy transitions, their importance has increased significantly. Ambitious EU decarbonization targets, coupled with rapid deployment of renewable energy, shape the traditional role of reserves within electricity markets. Renewable sources such as wind, solar and hydro, though essential for reducing greenhouse gas emissions, are inherently fluctuating, so less predictable compared to conventional generation. This fluctuation has increased the dependence on reserves, making them critical for securing system performance. Consequently, reserve services now represent a growing and increasingly important share of total electricity system costs, increasing the urgency of accurately allocation them within energy markets.

The complexity of modern power systems is further amplified by new patterns of electricity consumption and supply. The electrification of transport is expected to add substantial new load to the grid, especially as the adoption of electric vehicle accelerates across Europe. Data centers already consume 1.5–2% of global electricity under a constant load, and their expanding role, driven by AI and cloud computing, is projected to triple demand by 2030, creating local congestion and additional stress on distribution networks [1]. Together, these developments increase the pressure on system operators to secure sufficient balancing capacity while also responding to new demand patterns that differ from traditional industrial or residential loads.

At the same time, the gradual transition away from coal reduces the amount of flexible generation that made the system more adaptable. Natural gas plants, pumped-storage generation and emerging technologies such as battery storage are increasingly filling this role, but their availability and economics depend heavily on how reserve and grid-forming services are priced. Furthermore, the trade of electricity across borders within the EU adds another layer of complexity. Interconnected systems allow for more efficient sharing of resources, but also require consistent rules for acquiring and distributing reserves to avoid risks of inefficiency and reliability.

Despite the growing importance of reserves, much of the existing research on electricity markets has focused on structural models to analyze the implications of alternative market arrangements, as documented by foundational work on modeling trends [2] and price formation [3], [4]. While such approaches have been valuable in understanding market behavior, they often pay less attention to the detailed estimation of reserve allocation [6]. This oversight is becoming problematic as reserves are no longer a marginal component but rather a central factor in system operation. Underestimating their allocation could lead to suboptimal investment signals for the flexibility resources needed to support the energy transition.

This issue is particularly relevant in the European electricity market, where reserve prices are currently determined through a separate, sequential clearing mechanism. Under this methodology, the allocation of reserve capacity is calculated first, based on estimates of day-ahead energy prices, and subsequently, the allocation of actual energy production is determined. This two-step approach can introduce economic inefficiencies and potential pricing distortions due to neglecting the interdependent nature of energy and reserves. Specifically, since energy and reserves rely on the same limited generation and network capacity resources, ignoring their inherent coupling may lead to suboptimal allocation decisions and distorted price signals, as highlighted in the literature [7], [8].

In contrast, alternative market designs, like in the United States, co-optimize prices and quantities of energy and reserves through a multi-product auctions, acknowledging their interdependency. Such methods have consistently demonstrated significant economic benefits in terms of efficiency gains and reduced system operation costs. The Midcontinent ISO's adoption of co-optimization techniques, for example, has shown $2.1-3 billion in savings over the period 2007 to 2010, underscoring the potential value of shifting away from sequential market designs [9], [10].

Even with such evidence, the current European norm remains sequential market clearing, rooted historically in institutional structures, market governance, and preferences for portfolio-based bidding rather than centralized, unit-specific optimization. However, as European electricity markets become more integrated, these practices are being reconsidered. Recent European regulations, notably articles 40 and 41 of the European Balancing Guideline (EBGL), propose two main approaches: either fully integrating energy and reserves (co-optimization) or improving the existing sequential (market-based) system by enabling the exchange of reserves between countries [11]. These regulations aim to simplify international reserve trading and ensure efficient use of network capacity across Europe. Ultimately, their goal is to promote better resource allocation, lower costs, and improve consumer welfare.

2.2 Thesis Objective

Considering the critical context described above, the primary goal of this thesis is to systematically evaluate and compare the efficiency of sequential clearing methodologies of energy and reserve, against a fully integrated co-optimization approach. Furthermore, the analysis will differentiate between two forms of sequential clearing: a joint allocation of both reserve products (aFRR and mFRR) and the current European practice of separate, sequential clearing of aFRR followed by mFRR. To achieve this, the total cost of energy production is calculated for all methods, using corresponding mathematical models for each one. In doing so, the financial inefficiencies resulting from sequential clearing can be clearly identified.

The outcomes aim to inform the ongoing evolution of electricity market structures within Europe. By providing quantitative evidence on the comparative performance of these market designs, this work seeks to support policymakers, regulators, and industry stakeholders as they consider reforms to improve market efficiency, reliability, and integration. The insights generated may help identify best practices, highlight potential pitfalls of current approaches, and guide the adoption of more effective mechanisms for resource allocation.

Ultimately, the findings aim to contribute to the creation of a more resilient and cost-effective electricity system that is better equipped to meet the challenges of increasing renewable integration and evolving market needs. By providing measurable evidence, this work will contribute to a more resilient and cost-effective electricity system that is better equipped to meet the challenges of increasing renewable integration.

2.3 Methodological Overview

This thesis develops and implements a detailed mathematical framework to simulate and compare different market clearing mechanisms. The core of this methodology is a set of optimization models designed to capture the complex interdependencies between energy and reserve markets. By accounting for technical constraints of various generator types, including ramping limits, minimum up/down times, and start-up costs, the models provide a realistic representation of a power system. These models are implemented in Julia, taking advantage of its efficiency for computationally intensive problems, and solved using Gurobi.

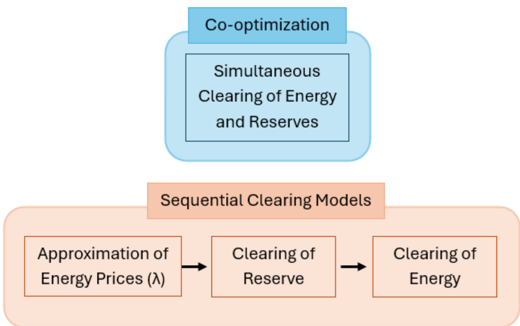

Figure 2.1: The two main approaches to power market clearing: Sequential Clearing versus Co-optimization

The analysis focuses on three distinct market designs:

- **Co-optimization:** A single, integrated model that clears energy and all reserve products simultaneously.
- **Sequential Clearing with Joint Reserves:** A multi-step model where energy prices are first approximated, followed by a simultaneous clearing of both reserve products (aFRR and mFRR), and a final energy allocation step.
- **Sequential Clearing with Separate Reserves:** A similar multi-step approach, but with a separate clearing of each reserve product individually (aFRR first, then mFRR), before the final energy allocation.

By simulating a realistic case study of the Belgian power system, this work calculates the total system cost for each of the three models and provides comparative plots of technology allocation in energy generation and reserves. This analytical comparison allows for the precise identification of financial inefficiencies, and their origins, that result from the different sequential clearing designs.

2.4 Related Literature

The literature analyzing electricity market design stands at the intersection of power system engineering and microeconomic theory, aimed at achieving reliable and economically optimal operation under conditions of increasing uncertainty. This review provides the foundation for analyzing the Clearing of Reserve and Energy Markets with Multiple Reserve Products by comparing integrated and sequential clearing approaches, the specific modeling complexities they introduce and the policy solutions emerging from contemporary research.

2.4.1 Structural Modeling and VRE Integration

The use of structural models, with extensive optimization frameworks, is a common approach in academic literature to determine the effects of electricity market restructuring. Such models have been instrumental in assessing the role of market power in the California's market restructuring [12], quantifying the efficiency and distributional effects of Colombia's shift to centralized unit commitment [13] and evaluating the impact of scarcity pricing on the fluctuation of flexible resources in Belgium [14].

The massive integration of Variable Renewable Energy (VRE) sources profoundly challenges traditional structural modeling efforts, requiring increased detail in input data and improved modeling of market behavior. This high VRE penetration introduces significant uncertainty, which, in turn, requires faster and with higher capacity reserve services than previously used. Consequently, effective advanced techniques for managing this uncertainty are crucial, necessitating complex reserve categorization, such as the aFRR and mFRR products [15] that are central to the European balancing market.

This structural shift means that the capacity and coordination of flexible resources, like the pumped-storage hydro assets central to the Belgian system, have become paramount for ensuring system stability. To address this, the Dynamic Dimensioning Approach for Operating Reserves [16] offers a practical, data-driven framework. Successfully testing the approach in the Belgian power system explicitly proved the need for dynamic, data-driven frameworks to replace outdated, static methods for sizing reserves.

2.4.2 Co-optimization versus Sequential Clearing

A growing conflict in market design revolves around synchronizing the optimization of energy and reserve markets. Co-optimization, where the quantities for energy and all reserve products are determined simultaneously, is widely recognized as the economically efficient method [17]. This superiority results from the model's ability to accurately price opportunity costs, which means that resources committed to provide products of high value, like fast reserves (aFRR), bear an explicit cost that is directly reflected in all market dispatch decisions. In this integrated approach, the system's optimization problem simultaneously determines if a megawatt-hour is more valuable as energy or as reserve capacity, thus forcing the market clearing price of the cheaper product to rise until it accurately compensates the generator for forgoing the more expensive alternative. This simultaneous optimization minimizes the total system cost [18].

Despite this clear advantage of co-optimization, the European system primarily employs sequential clearing. This process requires a subsequent approach where reserves are allocated first, based on approximated day-ahead energy prices, followed by the final energy allocation. This separation leads to systemic inefficiencies, creating inaccurate price signals and suboptimal allocation decisions due to the negligence of the critical interconnection between energy and reserve capacity [7], [19]. This issue is particularly ironic given that the European day-ahead market already operates as a multiple-product auction, simultaneously clearing interdependent transmission capacity and energy [20].

The theoretical advantage of the integrated approach is confirmed by empirical evidence from markets that use co-optimization, such as those in North America. These markets avoided intermediate sequential clearing phases and instead directly adopted multi-product auction mechanisms for simultaneous energy and reserve trading [18]. Studies focusing on markets such as the Alberta Electric System Operator (AESO) analyze clear, practical cost differences and superior price formation resulting from co-optimized clearing [21], [22]. This body of work validates the hypothesis that integrated clearing mechanisms consistently deliver lower total system costs compared to sequential designs [17].

The reliance of Europe's market design on sequential clearing methodologies, despite this evidence, originates from historical and institutional structures. However, as the European electricity system becomes more integrated and renewable penetration increases, these structural inefficiencies pose a growing financial threat, presenting a substantial research opportunity that this thesis aims to address quantitatively.

2.4.3 Modeling Complexities and European Regulatory Context

The comparative analysis of sequential versus co-optimized clearing presents unique methodological challenges that have received insufficient attention in current structural modeling literature. Two fundamental issues must be resolved:

1. **Fixed Costs and Ramping Constraints: Managing startup expenses and minimum load operational requirements** creates substantial complications within sequential market frameworks. These temporary fixed costs do not have a clear separation between reserve and energy market components [23],[24]. Furthermore, ramping rate limitations introduce considerable complexity, often requiring advanced analytical frameworks such as Lagrange relaxation methods for systematic cost distribution and ramping constraint management.

2. **Opportunity Cost Modeling in Reserve Clearing:** Reserve market bidding necessitates forecasting the opportunity costs of reserve provision [25], which fundamentally relies on energy price predictions. Academic research indicates that convex hull pricing structures [26] offer optimal price signals for opportunity cost study in day-ahead reserve markets, a principle leveraged in the co-optimization approach.

Furthermore, this research is motivated by ongoing European electricity market reforms. The European Balancing Guideline (EBGL) and recent ENTSO-E reports demonstrate that while the EU is working to harmonize and integrate balancing markets, for example through platforms like MARI and PICASSO, the core market structure remains sequential. This thesis provides critical quantitative evidence to inform policymakers about the financial toll of maintaining this sequential design.

Resent research demonstrates the need for market solutions that facilitate cross-border efficiency, a crucial component of the European internal energy market. Work by Backer [27] focuses on cross-border integration effects and the role of coordination in maximizing resource use across regions. The challenges of multi-area reserve sizing, tackled through advanced mathematical formulations like Multi-Area Reserve Dimensioning Using Chance-Constrained Optimization [28], underscore the need for sophisticated, integrated models when expanding the scope of the market.

Also, research [29] analyzes the limitations of current European approaches, explicitly advocating for real-time reserve pricing and scarcity mechanisms to address the "missing market" problem, an approach further formalized in Market Design Considerations for Scarcity Pricing: A Stochastic Equilibrium Framework [30]. These works provide the necessary policy context for arguing that co-optimization is a critical structural reform for ensuring that flexible resources are appropriately valued and sustained in a system increasingly dominated by renewable generation.

Finally, the practical application of these complex structural models, especially in the European context, relies on high-performance computing. Consequently, the co-optimization and sequential clearing models presented here are simplified versions derived from the methodological framework of Papavasiliou and Ávila [31]. The pumped-storage hydro formulations follow established modeling conventions for unit commitment in Belgium [14].

Chapter 3

Methodology

3.1 Study Objective

The primary objective of this study is to systematically analyze and determine the efficiency of different market clearing methodologies. It aims to compare the total system cost and resource allocation under co-optimized and sequential market designs. Through the application of detailed mathematical models to the Belgian power system, this work seeks to provide empirical evidence of the financial and operational benefits of co-optimization. The findings will serve as a crucial input for ongoing discussions about the design of future electricity markets in Europe, helping to inform policymakers and regulators as they seek to improve market efficiency, reliability, and the integration of renewable energy sources.

3.2 Modeling Framework

This section introduces the mathematical modeling framework used to simulate and analyze the market clearing mechanisms. The models are built on a set of core assumptions and parameters that define the characteristics of the power system and its components.

3.2.1 Time Steps, Day Types and Seasons

The modeling framework uses a representative day approach to analyze the efficiency of different market designs over a full year without needing to simulate every hour, which is computationally impractical. This method allows for a detailed, high-resolution analysis of operational dynamics.

The model's core divides each simulated day into 96 time steps of 15 minutes, matching the structure of the input data. This level of detail is essential for accurately capturing short-term operational factors, such as generator ramping limits and the rapid response required by reserve products. The analysis incorporates eight distinct operating scenarios, which are necessary to capture the full spectrum of operational challenges encountered annually. These scenarios are defined by two key temporal dimensions: weekday vs. weekend day types, which account for significant differences in daily load profiles, and four distinct seasons (autumn, winter, spring, summer), which capture seasonal variations in electricity demand and renewable production profiles.

The total yearly system cost for each market clearing methodology is subsequently derived by using the calculated production costs from these representative days to estimate the annual total. This process allows the thesis to quantify the systemic annual inefficiencies introduced by sequential clearing designs based on a detailed examination of critical operating periods.

3.2.2 Energy Generation

In the model, generator units reflect the actual Belgian generation fleet and are defined not only by their fuel type but also by the operational and economic constraints that shape their role in the market clearing process. The diverse generation mix is essential to ensure system reliability and determine the total cost of energy production.

Conventional and Flexible Generation

- **Thermal Units** including natural gas, gasoil and biomass primarily function as a source of dispatchable generation, covering mid-merit load. Critically, they are also a key resource for reserve supply, both aFRR and mFRR depending on their up and down ramp rates, due to their ability to modulate output. Their operation, however, is complicated by nonconvex constraints, such as start-up costs, minimum up/down times, and restrictive ramp rate limits. These factors introduce fixed costs that are difficult to allocate between energy and reserve, highlighting a core inefficiency that the sequential clearing models must address.

- **Nuclear Generation** provides reliable, extensive baseload energy production. Because of the technology's design and operating parameters, like their slow ramp rate, these units are characterized by very low flexibility and are generally not used for reserve services. They are modeled as a stable, near-constant power injection, with their main impact on the market being the reduction of net load that other generators must meet.

- **Pumped-Storage Hydro (PSH)** is a highly flexible asset that stores energy by pumping water to an upper reservoir and generates electricity by releasing that water through turbines. It is a vital source of reserve, offering rapid response and high capacity for grid stability. PSH's operation is governed by complex dynamics, including reservoir storage level constraints, pumping/generating capacities, and the inherent efficiency factor (η).

Fluctuating Generation

- **Variable Renewable Energy Sources (RES)**, which include Wind, Solar and Run-of-River Hydro units, are essential for energy production to meet decarbonization targets. Their output, which is irregular and less predictable, is treated as a fixed, must-take energy injection based on historical data. They are generally not used for reserves and their inherent fluctuation, which creates unpredictable supply gaps, is the primary driver behind the increased and critical demand for more reserve products.

3.2.3 Reserve Products

Reserve products are specialized grid services that maintain the continuous balance between electricity supply and demand, ensuring that the frequency and voltage of the system remain stable. In the Belgian case study, the model focuses on two types of reserve:

- The **automatic Frequency Restoration Reserve (aFRR)** provides the fastest and most continuous adjustment to maintain the balance between electricity supply and demand in real time. This reserve is activated automatically by the Transmission System Operator's control system, typically within seconds, making it essential for stabilizing frequency. It is required to manage rapid, small-scale, and unexpected imbalances that constantly occur across the grid, acting as the grid's fastest shock absorber. The resources providing aFRR must be highly agile and capable of quick power modulation. In the sequential clearing model, the one also used in Europe, the aFRR market is prioritized.

- The **manual Frequency Restoration Reserve (mFRR)** provides a slower, but often more significant, response to frequency deviations that persist after the aFRR is activated. Activation is manual and designed to sustain power changes for a longer duration, typically in the range of 10 to 30 minutes. The primary role of mFRR is to restore the system frequency to its nominal value and to replenish the faster-acting aFRR. Because of its slower response time, in the window of 15 minutes for activation, a wider range of resources can participate in mFRR compared to aFRR. In the sequential clearing approach, the decision for mFRR allocation is constrained by the generator capacity that has already been committed to the faster aFRR service.

Both aFRR and mFRR are further divided into two types:

- **Upward Reserves**: These are activated when there is a sudden shortfall in supply (e.g. a power plant trips offline or a wind farm's output unexpectedly drops). Upward reserves increase generation or reduce load to bring the system's frequency back into balance.

- **Downward Reserves**: These are activated when there is an excess of generation relative to demand (e.g. due to an unexpected drop in consumption or an increase in wind or solar power output). Downward reserves decrease generation or increase load, in this modeling with storage through pumping, to absorb the surplus energy and prevent the frequency from rising too high.

3.3 Nomenclature

This section provides definitions for the sets, parameters, and variables used throughout this report. Given the highly technical nature of power systems modeling, these conventions ensure clarity and precision when discussing the various control mechanisms and different products.

Sets:

G Set of generation units, indexed by g

G_h Set of pumped-storage generation units, indexed by g

T Set of time periods, indexed by t

Parameters:

- MC_g Marginal cost of generator g [€/MWh]
- S_g Start-up cost for generator g [€]
- $VOLL$ Value of Lost Load (cost of unmet demand) [€/MWh]
- D_t Total energy demand at time t [MW]
- P_g^-, P_g^+ Minimum and maximum generation of g [MW]
- η Efficiency factor for pumped-storage hydro [–]
- $R_g^{+/-}$ Maximum ramp-up/ramp-down rate of generator g [MW/min]
- $R^{+/-aFRR}$ Total system requirement for aFRR (up/down) [MW]
- $R^{+/-mFRR}$ Total system requirement for mFRR (up/down) [MW]
- $DT^{+/-aFRR}$ Delivery time for aFRR (up/down) [min]
- $DT^{+/-mFRR}$ Delivery time for mFRR (up/down) [min]
- UT_g, DT_g Minimum Up/Down Time for generator g [min]
- P_S, P_W, P_{RoR} Estimates of energy production from Solar, Wind, and Run-of-River Hydro [MW]
- Ph_g^+ Maximum generation capacity of the pumped-storage hydro unit [MW]
- RP Maximum ramp-rate for pumped-storage hydro generation [MW/min]
- RD Maximum ramp-rate for pumped-storage hydro pumping [MW/min]

- ES Maximum Energy Storage capacity of the reservoirs [MW]
- λ_t Approximated Energy Price (Dual Multiplier of the energy balance constraint) [€/MWh]

Variables:

- p_{gt} Energy production of generator g at time t [MW]
- w_{gt} Commitment state of generator g at time t (**1** if *ON*, **0** if *OFF*) [Binary]
- z_{gt} Start-up decision for generator g at time t (**1** if *starts up*) [Binary]
- ls_t Lost Load (unmet energy demand) at time t [MW]
- ph_t Generation (power output) from pumped-storage hydro total generation at time t [MW]
- dh_t Pumping (storage input) for pumped-storage hydro total generation at time t [MW]
- e_t Energy storage level of the reservoirs at the end of time t [MW]
- $s_{gt}^{+/-aFRR}$ aFRR reserve capacity (up/down) provided by generator g [MW]
- $s_{gt}^{+/-mFRR}$ mFRR reserve capacity (up/down) provided by generator g [MW]
- $sh_t^{+/-aFRR}$ aFRR reserve capacity (up/down) provided by pumped-storage hydro total generation at time t [MW]
- $sh_t^{+/-mFRR}$ mFRR reserve capacity (up/down) provided by pumped-storage hydro total generation at time t [MW]

3.4 Co-Optimization

The co-optimization model represents a single, integrated optimization problem that simultaneously determines the optimal schedules and allocation across energy and all reserve markets, concluding in a common energy price for both. A key advantage of this comprehensive approach is its ability to model the power system as a unified resource allocation problem, which is essential to inherently account for the opportunity cost associated with committing limited generation capacity to a specific market product. However, this results in a complicated mathematical structure, connecting energy production variables with their reserve counterparts.

3.4.1 The mathematical Model

The mathematical model of the co-optimization method is described below.

$$z_{co} = \min_{p,\,s,\,w,\,z} \{\frac{1}{4}\sum_{t\in T_{15}}\sum_{g\in G} MC_g \cdot p_{gt} + \sum_{t\in T_{60}}\sum_{g\in G} S_g \cdot z_{gt} + \frac{1}{4}\sum_{t\in T_{15}} VOLL \cdot ls_t\} \quad (3.1)$$

$$\text{s.t.} \quad D_t = P_S + P_W + P_{RoR} + ph_t - dh_t + \sum_{g\in G} p_{gt} + ls_t \quad (3.2)$$

$$R^{-/+aFRR} = \sum_{g\in G} s_{gt}^{-/+aFRR} + sh_t^{+/-aFRR} \quad (3.3)$$

$$R^{-/+aFRR} + R^{-/+mFRR} = \sum_{g\in G} s_{gt}^{-/+mFRR} + \sum_{g\in G} s_{gt}^{-/+aFRR} +$$

$$+ sh_t^{+/-mFRR} + sh_t^{+/-aFRR} \quad (3.4)$$

$$s_{gt}^{-/+aFRR} \leq \min\{P_g^+, DT^{-/+aFRR} \cdot R_g^{-/+}\} \quad (3.5)$$

$$s_{gt}^{-/+mFRR} \leq \min\{P_g^+, DT^{-/+mFRR} \cdot R_g^{-/+}\} \quad (3.6)$$

$$p_{gt} + s_{gt}^{+mFRR} + s_{gt}^{+aFRR} \leq P_g^+ \cdot w_{gt} \quad (3.7)$$

$$p_{gt} - s_{gt}^{-mFRR} - s_{gt}^{-aFRR} \geq P_g^- \cdot w_{gt} \quad (3.8)$$

$$p_{gt} - p_{g,t-1} + s_{gt}^{+mFRR} + s_{gt}^{+aFRR} \leq 15 \cdot R_g^+ \quad (3.9)$$

$$p_{g,t-1} - p_{gt} + s_{gt}^{-mFRR} + s_{gt}^{-aFRR} \leq 15 \cdot R_g^- \quad (3.10)$$

$$g \in G$$

$$ph_t + sh_t^{+mFRR} + sh_t^{+aFRR} \leq \sum_{g\in Gh} Ph_g^+ \quad (3.11)$$

$$dh_t + sh_t^{-mFRR} + sh_t^{-aFRR} \leq \sum_{g\in Gh} Ph_g^+ \quad (3.12)$$

$$e_t = 0, t \in \{1, 25, 49, ...\} \quad (3.13)$$

$$e_t = e_{t-1} + \eta \cdot dh_{t-1} - ph_{t-1} \quad (3.14)$$

$$ph_t - ph_{t-1} + sh_t^{+mFRR} + sh_t^{+aFRR} \leq 15 \cdot RP \quad (3.15)$$

$$ph_t - ph_{t-1} - sh_t^{-mFRR} - sh_t^{-aFRR} \leq -15 \cdot RP \quad (3.16)$$

$$dh_t - dh_{t-1} + sh_t^{-mFRR} + sh_t^{-aFRR} \leq 15 \cdot RD \quad (3.17)$$

$$dh_t - dh_{t-1} - sh_t^{+mFRR} - sh_t^{+aFRR} \leq -15 \cdot RD \quad (3.18)$$

$$e_t \leq ES \quad (3.19)$$

$$w_{gt}, z_{gt} \in UC_g \quad (3.20)$$

$$p_{gt}, s_{gt}, z_{gt}, ph_{gt}, dh_{gt}, e_{gt}, sh_{gt} \geq 0, w_{gt} \in \{0, 1\} \quad (3.21)$$

where

$$UC_g = \{ \sum_{q=t-UT_g+1}^{t} z_{gq} \leq w_{gt}, g \in G, t \geq UT_g$$

$$\sum_{q=t+1}^{t+DT_g} z_{gq} \leq 1 - w_{gt}, g \in G, t \leq N - DT_g$$

$$z_{gt} \leq 1, g \in G, t \in T_{60}$$

$$z_{gt} \geq w_{gt} - w_{g,t-1}, g \in G, t \in T_{60}\}$$

3.4.2 Explanation of the Model

The objective function and constraints described below detail how the co-optimization model determines the optimal schedule for energy production and reserve allocation by unifying all operational variables into a single problem.

Equation (3.1) presents the objective function of the model, which minimizes the total system cost, comprising the cost of production, the start-up cost and value of lost load (VOLL) for unmet demand.

The constraint set begins with the energy balance constraint (3.2). In it, the total hourly demand (D_t) is satisfied by the production of wind (P_W), solar (R_S), row-of-river hydro (R_{RoR}), production (ph_t) and storage (dh_t) from pumped-storage hydro reservoirs, conventional generation (p_t) and the calculated lost load(ls_t). Critically, this constraint's dual variable is what defines the market clearing energy price (λ) in a co-optimization model. The market clearing conditions for reserves are represented in constraints (3.3) for the aFRR market and (3.4) for the mFRR market and help enforce the grid stability requirements. Constraint (3.3) ensures the aFRR requirement is met, securing fast acting frequency stability. Constraint (3.4) models the cascading nature of reserves, ensuring the combined aFRR and mFRR capacity meets the total system requirement, which is vital for sustained frequency restoration.

The physical limits on generation are managed by several critical constraints. Ramp rates limits (3.5) and (3.6) ensure the committed reserve capacity is physically deliverable within the reserve product's required delivery time ($DT^{-/+aFRR/mFRR}$), enforcing technical feasibility. Capacity limits (3.7) and (3.8) manage resource scarcity and technical minima of each unit. (3.7) ensures energy production plus total upward reserve commitment does not exceed the unit's maximum capacity (P^{+}), while (3.8) guarantees that energy production minus total downward reserve commitment does not fall below the unit's minimum run capacity (P^{-}). The Ramping Limits (3.9) and (3.10) manage operational security by ensuring that the transition between energy schedules (from the current dispatch to full reserve activation) is physically achievable within the 15-minute time step.

The set of constraints, (3.11) to (3.19), models pumped-storage hydro, and the variables used represent the aggregated behavior of this technology. As a highly flexible asset, pumped-storage hydro is a vital source of reserve, and these constraints are essential for accurately modeling its ability to offer rapid response and high capacity for grid stability. Its time dependence means that optimization decisions regarding pumped-storage hydro generation or pumping in the current period directly influence its availability and cost in future periods. Specifically, the constraint (3.11) limits combined hydro production and the upward reserve provision to not exceed the maximum generation capacity. Similarly, (3.12) restricts pumping operation together with downward reserves to remain within pumping capacity. Constraints (3.13) and (3.14) define the energy storage level of the reservoirs over time, setting initial conditions and modeling the energy balance evolution over time considering generation, pumping, and efficiency factors (η). Constraints (3.15) through (3.18) describe ramping limitations for pumped-storage units, ensuring that changes in pumping and generation operations between consecutive periods, including reserve commitments, remain within the 15-minute ramping capabilities. Constraint (3.19) limits the energy storage level to the maximum storage capacity. Finally, the unit commitment constrain (3.20) incorporates the generator commitment logic, including start-up procedures and minimum operational/shut-down time requirements. These formulations ensure that the dispatch decision is realistic and accounts for resource dependency across time.

3.5 Sequential approximation, clearing both reserves at the same time

In sequential clearing, optimization of the energy price is performed in three steps. First, the energy price λ is approximated. Then the two types of reserve, aFRR and mFRR, are cleared simultaneously, using the evaluated λ. Lastly, the need for energy production is calculated alongside the cost of production, considering the reserve values from the reserve clearing as parameters in the co-optimization model, taking out constraints that consider only reserves' variables.

3.5.1 Approximation of the day ahead energy prices

The sequential clearing approach separates the clearing of the Reserve and Energy markets, forcing the market to make a two phase decision one piece at a time, instead of simultaneously finding the most cost effective solution to deliver both products. This separation, which is common in European markets, creates significant methodological challenges. Estimating the opportunity cost of providing reserves is tricky and, in order to calculate it, the model requires an initial estimate of the energy market price, λ, for each time period t, which itself is challenging to determine.

In this thesis, this challenge is addressed by employing a practical approximation method to estimate the day-ahead energy price. This method assumes that the market operator can achieve a near optimal economic dispatch by relaxing the restrictive binary commitment constraint in the full co-optimization model, described in Section 3 .4, to a continuous variable $w_{gt} \in [0, 1]$.

By solving this convex problem, a simplified energy market outcome is obtained very quickly. The resulting dual variable associated with the Energy Balance Constraint (3.2) is then extracted for each time step t. This dual variable, λ_t, represents the marginal cost of supplying one additional unit of energy (MW) at that specific time period t.

Crucially, this approximation aims to simulate a market without any forecast errors. By counting on a λ_t derived from a perfect foresight model for the reserve clearing decision, we isolate the structural inefficiencies caused purely by the sequential nature of the market design, ignoring the price forecasting uncertainties in the real world. This fixed value of λ_t is subsequently treated as a known constant in the objective function of the reserve clearing models, in Sections 3.5.2 and 3.6.1, to accurately calculate the opportunity cost for reserve provision.

3.5.2 The mathematical Model

The calculation of the need for reserves is made according to the following mathematical model.

$$
\begin{aligned}
r(\lambda) = &\sum_{t\in T_{15}} \lambda_t \cdot D_t + min_{s,w,z}\{\sum_{g\in G} RCF_g(s_g, w_g; \lambda)+\\
&+\sum_{t\in T_{60}}\sum_{g\in G} S_g \cdot z_{gt}\} && (3.22)\\
\text{s.t.}\quad & R^{-/+aFRR} = \sum_{g\in G} s_{gt}^{-/+aFRR} + sh_t^{+/-aFRR} && (3.23)\\
& R^{-/+aFRR} + R^{-/+mFRR} = \sum_{g\in G} s_{gt}^{-/+mFRR} + \sum_{g\in G} s_{gt}^{-/+aFRR}+\\
& + sh_t^{+/-mFRR} + sh_t^{+/-aFRR} && (3.24)\\
& s_{gt}^{-/+aFRR} \leq \min\{P_g^+, DT^{-/+aFRR} \cdot R_g^{-/+}\} && (3.25)\\
& s_{gt}^{-/+mFRR} \leq \min\{P_g^+, DT^{-/+mFRR} \cdot R_g^{-/+}\} && (3.26)\\
& s_{gt}^{+mFRR} + s_{gt}^{+aFRR} + s_{gt}^{-mFRR} + s_{gt}^{-aFRR} \leq \{P^+ - P^-\} \cdot w_{gt} && (3.27)\\
& g \in G\\
& Ph_t + sh_t^{+mFRR} + sh_t^{+aFRR} \leq \sum_{g\in Gh} Ph^+ && (3.28)\\
& Dh_t + sh_t^{-mFRR} + sh_t^{-aFRR} \leq \sum_{g\in Gh} Ph^+ && (3.29)\\
& Ph_t - Ph_{t-1} + sh_t^{+mFRR} + sh_t^{+aFRR} \leq 15 \cdot RP && (3.30)\\
& Ph_t - Ph_{t-1} - sh_t^{-mFRR} - sh_t^{-aFRR} \leq -15 \cdot RP && (3.31)\\
& Dh_t - Dh_{t-1} + sh_t^{-mFRR} + sh_t^{-aFRR} \leq 15 \cdot RD && (3.32)\\
& Dh_t - Dh_{t-1} - sh_t^{+mFRR} - sh_t^{+aFRR} \leq -15 \cdot RD && (3.33)\\
& w_{gt}, z_{gt} \in UC_g && (3.34)\\
& p_{gt}, s_{gt}, z_{gt}, ph_{gt}, dh_{gt}, e_{gt}, sh_{gt} \geq 0, w_{gt} \in \{0,1\} && (3.35)
\end{aligned}
$$

where

$$
\begin{aligned}
RCF_{gt}(s_{gt}, w_{gt};\lambda) = & && (3.36)\\
= &\begin{cases} 0, & \text{if } w_{gt} = 0\\ (\frac{MC_g}{4} - \lambda) \cdot (P_g^- + s_{gt}^{-mFRR} + s_{gt}^{-aFRR}), & \text{if } w_{gt} = 1, (\frac{MC_g}{4} - \lambda) \geq 0\\ (\frac{MC_g}{4} - \lambda) \cdot (P_g^+ - s_{gt}^{+mFRR} - s_{gt}^{+aFRR}), & \text{if } w_{gt} = 1, (\frac{MC_g}{4} - \lambda) \leq 0 \end{cases}
\end{aligned}
$$

3.5.3 Explanation of the Model

The reserve clearing model (Equations (3.22) to (3.36)) forms the core of the sequential methodology and its primary function is to optimally allocate both aFRR and mFRR capacity across available generators.

The objective function (3.22) is calculated considering the estimated λ_t as a constant and minimizes the system cost, which is structured as the sum of the estimated cost of serving the demand, the total Realistic Cost Function (RCF) and the generator Start-up Costs.

The RCF, defined in (3.36), is vital for capturing the opportunity cost. It represents the potential profit (or loss) a committed generator g would incur if it were only generating energy, relative to the approximated market price λ_t.

- If the generator is out-of-the-money (its Marginal Cost is higher than λ_t), the RCF penalizes the unit by assuming it generates at its minimum load ($P_g^- + s_{gt}^{-mFRR} + s_{gt}^{-aFRR}$). This incentivizes the unit to shut down ($w_{gt} = 0$) unless its capacity is critically needed for reserve provision.
- If the generator is in-the-money (its Marginal Cost is lower than λ_t), the RCF rewards the unit by assuming it generates at its maximum capacity ($P_g^+ - s_{gt}^{+mFRR} - s_{gt}^{+aFRR}$). This encourages the low-cost unit to commit.

By minimizing this objective, the model selects the unit commitment schedule (w_{gt},z_{gt}) and reserve allocation (s_{gt}) that minimizes the cost of providing reserves, constrained by the estimated value of energy production.

Constraints (3.23) and (3.24) are in line with the market clearing conditions (3.3) and (3.4), ensuring the reserve balance. Constraints (3.25) and (3.26) apply ramp rate limitations as in (3.5) and (3.6) specifically for reserves. Constraint (3.27) ensures that reserve allocation lies within the generation margin defined by the upper and lower limit of each unit, extending the limits in (3.7) and (3.8).

From constraint (3.28) to (3.33) they are equivalent to their counterparts form the co-optimization model ((3.11) to (3.18)). Unlike the co-optimization model where pumped-storage generation and pumping are decision variables, here they are fixed parameters (Ph_t,Dh_t) derived from historical data (as modeled in your code). As a result the energy balance and storage dynamics constraints (3.13), (3.14) and (3.19) from the co-optimization are excluded here. The constraints now ensure that the reserve commitment (sh_t) respects the operating and ramping limits around this fixed historical schedule.

Constraint (3.34) refers to UC_g function, analyzed in the co-optimization formulation for the corresponding constrain (3.20).

3.5.4 Final Energy Dispatch

Following the commitment of reserve capacity, the sequential process concludes with a third, separate optimization step, the Energy Dispatch Model. This model determines the final energy production and calculates the total system cost. Critically, it incorporates the optimal reserve allocation values derived from this Reserve Clearing model as fixed capacity constraints on the unit's operating range. The generator's commitment state is not linked to the previous step because constraints (3.7) and (3.8) ensure it equals one whenever any reserve service (s_{gt}^{+FRR}, s_{gt}^{+aFRR}, s_{gt}^{-mFRR} or s_{gt}^{-aFRR}) is non zero. This step ensures that the final energy dispatch respects the capacity that has been locked in to provide reserve services to the grid.

3.6 Sequential approximation, clearing reserves separately

The energy clearing method currently implemented in European electricity markets differs slightly from the sequential model described in the previous section. In practice, different reserve types are settled in separate stages, with aFRR cleared first, followed immediately by mFRR. Although this procedure simplifies the clearing process at each stage, it simultaneously introduces additional inefficiencies in the overall energy allocation.

The the day ahead energy price approximation and the final energy dispatch are consistent with the methodology presented in Section 2.5. The only difference lies in the reserve allocation, which requires further expansion and will be detailed below.

3.6.1 The mathematical Model

The following mathematical formulations describe the separate allocation of the two reserve types. The first considers only aFRR, while the second incorporates the outcome of the first as input for the subsequent mFRR allocation.

The following considers the clearing of aFRR.

$$
\begin{aligned}
r^{aFRR}(\lambda) = & \sum_{t \in T_{15}} \lambda_t \cdot D_t + min_{s,w,z} \sum_{g \in G} RCF^{aFRR}_{gt}(s_g, w_g; \lambda) \\
& + \sum_{t \in T_{60}} \sum_{g \in G} S_g \cdot z_{gt} && (3.37) \\
\text{s.t.} \quad & R^{-/+aFRR} = \sum_{g \in G} s^{-/+aFRR}_{gt} + sh^{+/-aFRR}_t && (3.38) \\
& s^{-/+aFRR}_{gt} \leq \min\{P^+_g, DT^{-/+aFRR} \cdot R^{-/+}_g\} && (3.39) \\
& s^{-/+aFRR}_{gt} \leq 15 \cdot R^{-/+}_g && (3.40) \\
& s^{+aFRR}_{gt} + s^{-aFRR}_{gt} \leq \{P^+ - P^-\} \cdot w_{gt} && (3.41) \\
& g \in G \\
& Ph_t + sh^{+aFRR}_t \leq \sum_{g \in Gh} Ph^+ && (3.42) \\
& Dh_t + sh^{-aFRR}_t \leq \sum_{g \in Gh} Ph^+ && (3.43) \\
& Ph_t - Ph_{t-1} + sh^{+aFRR}_t \leq 15 \cdot RP && (3.44) \\
& Ph_t - Ph_{t-1} - sh^{-aFRR}_t \leq -15 \cdot RP && (3.45) \\
& Dh_t - Dh_{t-1} + sh^{-aFRR}_t \leq 15 \cdot RD && (3.46) \\
& Dh_t - Dh_{t-1} - sh^{+aFRR}_t \leq -15 \cdot RD && (3.47) \\
& w_{gt}, z_{gt} \in UC_g && (3.48)
\end{aligned}
$$

$$p_{gt}, s_{gt}, z_{gt}, ph_{gt}, dh_{gt}, e_{gt}, sh_{gt} \geq 0, w_{gt} \in \{0,1\} \tag{3.49}$$

where

$$RCF_{gt}^{aFRR}(s_{gt}, w_{gt}; \lambda) = \tag{3.50}$$
$$= \begin{cases} 0, & \text{if } w_{gt} = 0 \\ (\frac{MC_g}{4} - \lambda) \cdot (P_g^- + s_{gt}^{-aFRR}), & \text{if } w_{gt} = 1, (\frac{MC_g}{4} - \lambda) \geq 0 \\ (\frac{MC_g}{4} - \lambda) \cdot (P_g^+ - s_{gt}^{+aFRR}), & \text{if } w_{gt} = 1, (\frac{MC_g}{4} - \lambda) \leq 0 \end{cases}$$

The following considers the clearing of mFRR.

$$\begin{aligned} r^{mFRR}(\lambda) = & \sum_{t \in T_{15}} \lambda_t \cdot D_t + min_{s,w,z} \sum_{g \in G} RCF_{gt}^{mFRR}(s_g, w_g; \lambda) \\ & + \sum_{t \in T_{60}} \sum_{g \in G} S_g \cdot z_{gt} & (3.51) \\ \text{s.t.} \quad & R^{-/+mFRR} + R^{-/+aFRR} = \sum_{g \in G} \{ s_{gt}^{-/+mFRR} + S_{gt}^{-/+aFRR} \} + \\ & + sh_t^{-/+mFRR} + Sh_t^{-/+aFRR} & (3.52) \\ & s_{gt}^{-/+mFRR} \leq \min\{P_g^+, DT^{-/+mFRR} \cdot R_g^{-/+}\} & (3.53) \\ & s_{gt}^{-/+mFRR} + S_{gt}^{-/+aFRR} \leq 15 \cdot R_g^{-/+} & (3.54) \\ & s_{gt}^{+mFRR} + S_{gt}^{+aFRR} + s_{gt}^{-mFRR} + S_{gt}^{-aFRR} \leq \{P^+ - P^-\} \cdot w_{gt} & (3.55) \\ & g \in G \\ & Ph_t + sh_t^{+mFRR} + Sh_t^{+aFRR} \leq \sum_{g \in Gh} Ph^+ & (3.56) \\ & Dh_t + sh_t^{-mFRR} + Sh_t^{-aFRR} \leq \sum_{g \in Gh} Ph^+ & (3.57) \\ & Ph_t - Ph_{t-1} + sh_t^{+mFRR} + Sh_t^{+aFRR} \leq 15 \cdot RP & (3.58) \\ & Ph_t - Ph_{t-1} - sh_t^{-mFRR} + Sh_t^{-aFRR} \leq -15 \cdot RP & (3.59) \\ & Dh_t - Dh_{t-1} + sh_t^{-mFRR} + Sh_t^{-aFRR} \leq 15 \cdot RD & (3.60) \\ & Dh_t - Dh_{t-1} - sh_t^{+mFRR} + Sh_t^{+aFRR} \leq -15 \cdot RD & (3.61) \\ & w_{gt}, z_{gt} \in UC_g & (3.62) \\ & p_{gt}, s_{gt}, z_{gt}, ph_{gt}, dh_{gt}, e_{gt}, sh_{gt} \geq 0, w_{gt} \in \{0,1\} & (3.63) \end{aligned}$$

where

$$RCF_{gt}^{mFRR}(s_{gt}, w_{gt}; \lambda) = \tag{3.64}$$
$$= \begin{cases} 0, & \text{if } w_{gt} = 0 \\ (\frac{MC_g}{4} - \lambda) \cdot (P_g^- + s_{gt}^{-mFRR} + S_{gt}^{-aFRR}), & \text{if } w_{gt} = 1, (\frac{MC_g}{4} - \lambda) \geq 0 \\ (\frac{MC_g}{4} - \lambda) \cdot (P_g^+ - s_{gt}^{+mFRR} - S_{gt}^{+aFRR}), & \text{if } w_{gt} = 1, (\frac{MC_g}{4} - \lambda) \leq 0 \end{cases}$$

3.6.2 Explanation of the Model

The separate clearing of aFRR (Equations (3.37) to (3.50)) follows exactly the mathematical formulation as the combined reserve model (Equations (3.22) to (3.36)), with the only modification being the removal of variables and constraints related to mFRR. The parameter λ is again treated as known and should have been approximated in a previous step.

The formulation for clearing the second reserve type, mFRR, (Equations (3.51) to (3.64)) closely mirrors that of the combined reserve model, except that the aFRR related parameters are introduced as predetermined constants.

3.7 Implementation in Julia

The optimization models formulated in Sections 3.4, 3.5, and 3.6 were computationally implemented using the Julia programming language. Julia was selected for its efficiency in handling large-scale numerical problems and its strong ecosystem for optimization, utilizing the Gurobi solver.

3.7.1 General Implementation Structure

To maintain simplicity, the models were applied to a case study of a single European country, Belgium. Therefore, the input data, including generation capacities, renewable profiles, load curves, reserve requirements, and cost parameters, were imported and filtered to include only the relevant Belgian generators and load profiles. The daily time horizon was divided into 96 periods (15-minute slots) , with a mapping array created to connect these 15-minute periods to the hourly binary unit commitment variables for a 24-hour cycle.

In order to get results for one specific day of the year, the required data for the energy demand profile and the renewable generation profiles, were chosen to match one distinct seasonal period (Autumn, Winter, Spring, or Summer) and one day type (Weekday or Weekend Day) for the simulation.

Each generator was defined by its different technology (natural gas, nuclear, wind, solar, hydro, etc.) to allow for technology based analysis. The energy production from wind, solar, and run-of-river hydro units was treated as fixed, based on the historical data available from previous years (2013 - 2014). The daily time horizon was divided into 96 periods (15-minute slots) and each generator's technical parameters, along with the reserve requirements, were stored in dictionaries.

For constraints involving interactions between two consecutive time periods, wrap-up constraints were introduced to link the end of the day with its beginning, ensuring a continuous 24-hour operation cycle.

During the implementation of the sequential clearing models in Julia, several formulation adjustments were necessary to ensure model solvability. The constraints causing infeasibility were identified through systematic debugging and, in some cases, suspected constraints were temporarily removed to find the source of infeasibility. For example, one of those constraints was the power balance constraint (Equation 3.2), which was reformulated to be equal to zero ($D_t - P_S - P_W - P_{RoR} - ph_t + dh_t - \sum_{g \in G} p_{gt} - ls_t = 0$) to resolve numerical issues and ensure feasible solutions.

Every model was solved using Gurobi and the solution provided optimal generator schedules, the cost of production and reserve allocations. To visualize these outcomes, the results were plotted as time series charts that display the 24 hour dispatch (96 periods) for each technology, separately illustrating the allocated capacity for energy generation, aFRR up/down reserves and mFRR up/down reserves.

3.7.2 Co-optimization

The co-optimization approach was the simplest to implement from a structural standpoint, as it required only a single optimization problem.

The model was built exactly according to the mathematical formulation (Equations (3.1) to (3.21)), where energy production (p_{gt}) and reserve provision ($s_{gt}^{-/+aFRR}$, $s_{gt}^{-/+mFRR}$) are determined simultaneously. The objective function was to minimize the total system cost, which includes the variable generation costs, the start-up costs and the value of lost load (VOLL) for unmet demand. The solver returned the optimal unit commitment schedule, energy production levels, reserve allocation by generator and the optimal cost of production. The results were subsequently extracted and visualized in plots to show the allocation of energy and reserve over time.

3.7.3 Sequential Designs

Implementing the sequential clearing models required a multistep approach that involved three, distinct optimization problems. The difference in the two methodologies was the second optimization, where the reserve allocation takes place.

Step 1: Energy Price Approximation (λ) This initial step was common to both sequential models. It determined an approximation of the energy price (λ_t) for each time period (t). This was achieved by solving the complete co-optimization model (Equations (3.1) to (3.21)) while relaxing the binary commitment variable (w_{gt}) to be continuous in the interval [0,1]. The dual variable of the energy balance Constraint (3.2) at each time step provided the necessary λ_t value, which was then used as a fixed constant in the subsequent optimizations of reserve clearing.

Step 2: Reserve Clearing The reserve allocation stage utilized the predetermined λ_t values to minimize the opportunity cost of providing reserve, alongside the fixed startup costs.

- **Joint Reserve Clearing (Model 2.5):** A single optimization problem (Equations (3.22) to (3.35)) determined the allocation for both aFRR and mFRR simultaneously. In this step, the energy production (Pht) and storage (Dht) values for pumped-storage hydro were drawn from historical data, treating them as given parameters for the reserve allocation stage.

- **Separate Reserve Clearing (Model 2.6):** This stage was split into two sequential optimizations, as described in the mathematical methodology.
  1. The aFRR market was cleared first (Equations (3.37) to (3.50)).
  2. The resulting aFRR allocations were then fixed and incorporated as predetermined constants ($S_{gt}^{-/+aFRR}$) into the second optimization problem, which solved for the mFRR allocation (Equations (3.51) to (3.64)). This structure models the constraint imposed on the slower reserve by the capacity already committed to the faster reserve.

Step 3: Final Energy Allocation The final optimization problem determined the definitive cost of energy production and the final energy allocation for all generators. The reserve allocations determined in Step 2 (either jointly or separately) were incorporated as fixed constraints on generator capacity. The results were stored and visualized in plots and the total annual cost was calculated for comparison with the other models.

3.8 Approximation of Annual system cost

The core objective of the efficiency analysis is to quantify the total system cost over a full year, C_{annual}, for each market clearing methodology. Since simulating all 365 days of the year is computationally strenuous, the total annual cost is derived by using the calculated production costs from a limited set of representative days, which are then extended for the whole year.

3.8.1 Nomenclature and Calculation

Each of the three models (Co-optimization, Sequential with Joint Reserves and Sequential with Separate Reserves) puts out the daily cost of energy production for a specific season (autumn, winter, spring or summer) and day type (weekday or weekend day) of the year. Afterwords the annual cost is calculated using the following equation.

$$C_{annual} = \sum_{\substack{s \in \{\text{FA, WI, SP, SU}\} \\ d \in \{\text{WD, WE}\}}} N_{s,d} \cdot C_{s,d} \tag{3.65}$$

where the terms are defined as:

C_{annual} The total estimated cost of energy generation for a full year [€]

$C_{s,d}$ The calculated daily system cost for the representative day of season s and day type d [€/Day]

$N_{s,d}$ The total number of days that are of the day type d and in season s in each year [Days]

This approach acknowledges that operational factors, such as generation schedules, reserve needs, and electricity demand, vary dramatically between weekdays and weekend days, and also due to seasonal weather patterns (e.g., higher winter demand, greater summer solar output). By multiplying the calculated, optimized cost of a single representative day ($C_{s,d}$) by its frequency ($N_{s,d}$), the model ensures that the resulting C_{Annual} accurately reflects the real mix of operational challenges faced over the year.

3.8.2 Determination of Quantities ($N_{s,d}$)

The numerical quantities used in this analysis are derived by determining the specific number of weekdays and weekend days that fall within each defined season for the model year.

For the purpose of standardization, the model year is defined as a common 365-day year, which requires specific assumptions regarding the seasonal distribution of days. Although the actual number of weekdays and weekend days varies from year to year, this thesis employs a consistent set of figures, as shown in Table 2.1.

This standardized modeling approach ensures that any observed seasonal variation does not attribute the specific weekly alignment of a historical year. This methodology intentionally maintains the exact annual totals of the average common year (365 total days, 261 weekdays, 104 weekend days) while assigning an equal and mathematically consistent number of 26 weekend days to each of the four seasons, preventing disproportionate weighting due to random calendar effects.

Season	**Total Days**	**Weekdays**	**Weekend Days**
Autumn	91	65	26
Winter	90	64	26
Spring	92	66	26
Summer	92	66	26

Table 3.1: Standardized Distribution of Days for the Common Model Year.

Resulting Equation: The equation uses the daily costs ($C_{s,d}$) multiplied by predetermined factors ($N_{s,d}$) to cover the 365 days of the year, based on the seasonal division and day types.

$$\begin{aligned} C_{annual} = & 65 \cdot C_{FA,WD} + 26 \cdot C_{FA,WE} + 64 \cdot C_{WI,WD} + 26 \cdot C_{WI,WE} + 66 \cdot C_{SP,WD} + \\ & + 26 \cdot C_{SP,WE} + 66 \cdot C_{SU,WD} + 26 \cdot C_{SU,WE} \end{aligned} \tag{3.66}$$

The abbreviations, used to represent the daily cost of the specific season and day type, are defined below.

The method presented here ensures that the comparison between the three market clearing methodologies is robust and systemic. While the optimization models precisely calculate the short-term inefficiencies on a critical day, the final C_{annual} value translates these daily operational gains or losses into a measurable economic

Abbreviation	**Meaning**
WD	Weekday
WE	Weekend Day
WI	Winter
SP	Spring
SU	Summer
FA	Fall (Autumn)

Table 3.2: List of abbreviations used in the methodology

metric. This metric serves as the primary basis for the thesis's conclusion regarding the financial benefits and overall efficiency of the Co-optimization approach over the two sequential clearing approaches.

Chapter 4

Case Study

4.1 Description of the Case Study

The methodological framework outlined in Chapter 3 is applied to a detailed model of the Belgian power system. This region is strategically important due to its ongoing energy transition and its reliance on a diverse generation fleet. The system is managed by the Transmission System Operator (TSO), Elia, and operates within the broader European electricity market, which currently employs a sequential clearing mechanism.

The modeling framework incorporates the system's key operational and structural characteristics, including a diverse generation mix and a critical reliance on flexible resources to manage increasing renewable intermittency. For the purpose of this analysis, network constraints and the exchange of reserve capacity between countries are ignored to focus exclusively on the inherent structural inefficiencies introduced by the market clearing mechanism itself.

4.1.1 Key System Characteristics for Market Modeling

The Belgian grid is characterized by a significant combination of stable nuclear baseload, highly flexible pumped-storage assets, and thermal generation, alongside growing intermittent renewable energy sources.

Table 4.1 presents the distribution of Pumped-Storage Hydro (PSH) generation capacity.

Generator	**Reference Value** (MW)
Hydraulic Pumped-Storage	
COO_A_1_H	158.0
COO_A_2_H	158.0
COO_A_3_H	158.0
COO_A_4_H	230.0
COO_A_5_H	230.0
COO_A_6_H	230.0
PLATETAILLE	144.0

Table 4.1: Pumped-Storage Hydro Generators' Characteristics

Pumped-Storage Hydro (PSH): The Coo and Platétaille power stations are central to system flexibility, providing large scale storage and rapid response reserve capacity. For the purposes of this model, their combined capacity of 1,368 MW is treated as a single unit because all the units share similar operating characteristics. The efficiency factor for pumped-storage hydro, η, is set at 0.9 and the maximum energy storage capacity of the reservoirs (ES) at 5.71 GW. The ramp rates (RP, RD) are represented jointly for all the PSH generators at 200 MW/min.

All nuclear and thermal generators are listed in Table 4.2, representing the core units of the Belgian generation fleet. This table provides essential operational and economic characteristics for each unit, specifically including minimum and maximum capacities (Min and Max Cap.) in MW, ramp rates in MW/min, same for both up and down (U/D), generator commitment restrictions (Min U and Min D time in hours) and the estimated marginal cost of energy production (Marg. Cost), in €/MWh. The Startup Cost is 0.00 € for every generator in the model, except for the natural gas unit AMERCOEUR_1, which has a non-zero Startup Cost of 11,903.56 €.

Generator	**Min Cap.** *(MW)*	**Max Cap.** *(MW)*	**Ramp U/D** *(MW/m)*	**Min U** *(hr)*	**Min D** *(hr)*	**Marg. Cost** *(€/MWh)*
Nuclear						
DOEL_1	216.30	432.50	14.41	168	168	7.58
DOEL_2	216.30	432.50	14.41	168	168	7.58
DOEL_3	503.00	1006.00	33.53	168	168	7.36
DOEL_4	522.00	1044.00	34.80	168	168	6.90
TIHANGE_1	481.00	962.00	32.07	168	168	7.36
TIHANGE_2	504.00	1008.00	33.60	168	168	7.58
TIHANGE_3	525.50	1051.00	35.03	168	168	7.58
Gasoil						
TURBOJETS_BE_VLG	42.00	140.00	1.40	3	2	226.21
TURBOJETS_BE_BRU	10.80	36.00	0.36	3	2	207.47
Biomass						
LANGERLO_2A_EON	20.60	258.00	2.58	12	8	21.16
RODENHUIZE_ _MAX_GREEN	17.20	215.00	4.30	12	8	64.97
RUIEN_3	10.40	130.00	1.30	12	8	33.67
RUIEN_4	9.80	122.00	1.22	12	8	34.35
Waste						
SCHAERBEEK	10.80	45.00	2.25	2	2	19.70
HERSTAL_UVELIA	7.20	30.00	1.50	2	2	0.00
INDAVER	4.80	20.00	1.00	2	2	36.45
ISVAG	2.50	10.50	0.52	2	2	26.07

Generator	**Min Cap.** (*MW*)	**Max Cap.** (*MW*)	**Ramp U/D** (*MW/m*)	**Min U** (*hr*)	**Min D** (*hr*)	**Marg. Cost** (*€/MWh*)
Natural Gas						
AMERCOEUR_1	240.40	437.00	13.11	8	4	40.23
SMALL_ _CHP_GAS_FLANDERS	0.00	543.00	10.86	0	0	49.52
SPE_CCGT_SERAING	266.80	485.00	14.55	8	4	46.76
HERDERSBRUG	264.20	480.30	14.41	8	4	42.54
DROGENBOS	253.00	460.00	13.80	8	4	46.70
TPOWER	231.00	420.00	12.60	8	4	44.57
DUFERCO_CCGT	225.50	410.00	12.30	8	4	40.62
VILVOORDE_EON	211.80	385.00	11.55	8	4	45.30
ZANDVLIET	270.00	375.00	15.00	8	4	46.71
SPE_CCGT_ _GENT_RINGVAART	192.50	350.00	10.50	8	4	46.72
STGHISLAIN	192.50	350.00	10.50	8	4	45.30
RUIEN_6	23.50	294.00	2.94	12	8	58.23
RUIEN_5A	23.20	290.00	2.90	12	8	62.19
LANGERLO_1A_EON	20.60	258.00	2.58	12	8	58.63
GENERIC_GT_B_Aubang_I	48.70	203.00	10.15	2	2	85.12
GENERIC_GT_B_Aubang_II	48.70	203.00	10.15	2	2	85.81
GENERIC_GT_B13_I	48.70	203.00	10.15	2	2	83.05
GENERIC_GT_B13_II	48.70	203.00	10.15	2	2	83.07
GENERIC_GT_B13_III	48.70	203.00	10.15	2	2	83.76
Blast Gas						
SIDMAR	280.00	305.00	1.67	12	8	19.66

Table 4.2: Conventional Generators' Characteristics

Nuclear Generation: This group provides the system's baseload energy, with a total maximum capacity of the modeled Doel and Tihange power plants at 5,630.5 MW. It is characterized by high minimum run capacities and low flexibility due to long minimum up/down times (UT_g/DT_g) of 168 hours. As a result, it is not commonly used as a reserve product.

Thermal Generation: These units, predominantly fueled by natural gas, are also primary sources for flexible energy dispatch and reserve provision due to their ability to modulate output quickly. The most representative thermal units modeled for the Belgian system include Combined Cycle Gas Turbines (CCGTs) such as TPOWER, DROGENBOS, and SPE_CCGT_SERAING, with high ramping capability and operational flexibility.

Generator	**Stations**	**Reference Value** (MW)
Solar (PV)	17	5,083.28431
Onshore Wind	17	2,371.87469
Offshore Wind	2	2,105.99307
Hydraulic Run-of-Rive	1	186.0

Table 4.3: Aggregated Renewable Generation Capacity

Renewable Energy Sources: Sources such as wind, including offshore capacity like WINDOFF_BELWIND and WINDOFF_CPOWER, solar and run-of-river hydro are treated as fixed energy injections and scaled by predefined multipliers specific to each season and day type to approximate realistic renewable generation profiles. This inherent fluctuation however, creates unpredictable supply gaps, driving unavoidably the increased and critical demand for flexible reserve.

In total, the installed capacity for the technologies included in the optimization models are:

- Natural Gas: 6,552.3 MW
- Nuclear: 5,936.0 MW
- Solar (PV): 5,083.3 MW
- Wind (Onshore & Offshore): 4,477.9 MW
- Pumped-Storage Hydro: 1,308.0 MW
- Biomass: 725.0 MW
- Blast Gas: 305.0 MW
- Run-of-River Hydro: 186.0 MW
- Gasoil: 176.0 MW
- Waste: 105.5 MW

This detailed representation of energy generation ensures that the analysis provides realistic insights into the comparative efficiency of co-optimization versus sequential market clearing in Belgium.

4.2 Analysis of Cost Inefficiencies

This section presents the main, numerical findings of the study by comparing the daily and annual system costs for the three market clearing models. These costs serve as the direct metric for determining the efficiency of co-optimization against the sequential designs. The daily cost results were extracted using the computational framework developed in Virtual Studio Code, where the methodologies were coded in Julia (as described in Section 3.7) and optimized using the Gurobi solver. This analysis measures the financial impact of structural market separation, highlighting the avoidable operational waste introduced by suboptimal resource commitment in the sequential models.

Month & Day Type	Co-optimization	Sequential with Joint Reserves	Sequential with Separate Reserves
Autumn-WD	2,171,680	2,248,550	2,248,416
Autumn-WE	1,116,137	1,225,743	1,225,800
Winter-WD	1,372,060	1,580,779	1,580,777
Winter-WE	828,047	1,045,128	1,045,177
Spring-WD	2,029,704	2,219,903	2,220,026
Spring-WE	1,322,172	1,547,376	1,547,380
Summer-WD	1,981,152	2,104,766	2,104,762
Summer-WE	1,404,564	1,584,777	1,584,811

Table 4.4: Daily Cost of Energy Production for Each Model in Different Seasons and Day Types

The stark differences in daily system costs across the market designs, as quantified in Table 4.4, are visually presented in the following figures. Figure 4.1(a) compares the system costs of the co-optimization approach against the sequential with joint reserve clearing. Similarly, Figure 4.1(b) juxtaposes the costs of the co-optimization model with the sequential with separate reserve clearing.

Figure 4.1: Comparative Daily System Cost Graphs of Co-optimization vs. Sequential Clearing Models

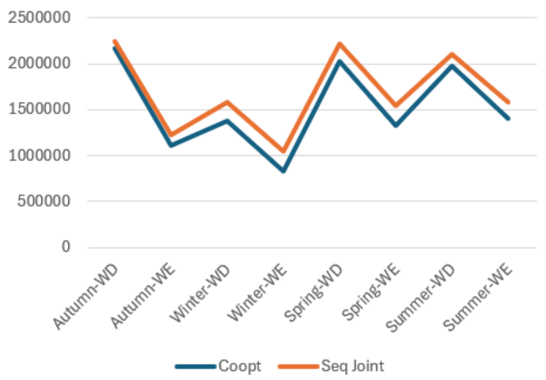

((a)) Co-optimization vs. Sequential Clearing with Joint Reserves

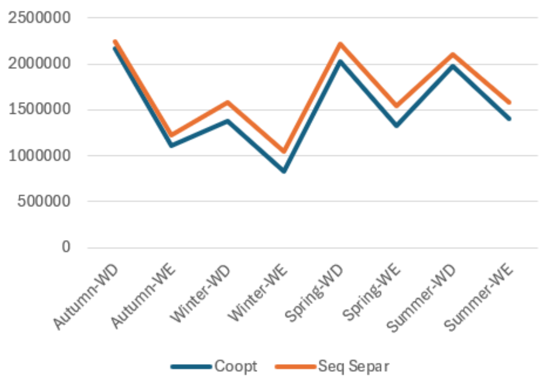

((b)) Co-optimization vs. Sequential Clearing with Separate Reserves

The structural inefficiencies inherent in the two sequential market clearing methodologies are expressed as a percentage deviation from the optimal outcome achieved by the co-optimization model. These results are presented in Table 4.5.

Month & Day Type	**Inefficiencies in Sequential - Joint Res.**	**Inefficiencies in Sequential - Separate Res.**
Autumn-WD	3.42 %	3.41 %
Autumn-WE	8.94 %	8.95 %
Winter-WD	13.20 %	13.20 %
Winter-WE	20.77 %	20.77 %
Spring-WD	8.57 %	8.57 %
Spring-WE	14.55 %	14.55 %
Summer-WD	5.87 %	5.87 %
Summer-WE	11.37 %	11.37 %

Table 4.5: Inefficiencies in both Sequential designs compared to Co-optimization

As shown in Table 4.5, throughout the year, inefficiencies in both sequential designs are substantial and vary by season and day type.

The highest cost increase is observed during the winter weekend day (Winter-WE) scenario, where both sequential with joint and separate reserve clearing show inefficiencies greater than 20%. This indicates that winter conditions (high demand and greater fluctuation) expose the sequential approach's inability to efficiently allocate limited flexible resources like natural gas and pumped-storage hydro.

Afterwords the annual cost of energy production can be calculated applying the data from Table 4.4 in equation 3.66. The results for each are shown bellow.

- $C_{annual}[Coopt] = 615,131,456$ €
- $C_{annual}[SeqJoint] = 673,232,384$ €
- $C_{annual}[SeqSep] = 673,235,144$ €

The financial inefficiency of the sequential joint reserve clearing is 8.63%, leading to a wastage of resources valued at $58,100,928$ € per year relative to the co-optimization benchmark. The sequential separate reserve clearing, which mirrors current European practice, is the most expensive option, resulting in an inefficiency of 8.63% and resulting in an annual excess cost of $58,103,688$ €.

The difference between the two sequential designs throughout the year is almost zero, accounting for less than 0.006% deviation in every day case. This becomes prominent in the annual calculation, as the tow designs have an almost zero difference, of 2,760 €, making the separate clearing of reserves slightly less financially efficient.

The clear escalation in system cost for both sequential models confirms that the structural separation of markets introduces significant inefficiencies, forcing suboptimal resource allocation and driving up the overall system operating cost compared to the optimal dispatch of the co-optimization model.

4.3 Reserve and Energy Allocation

Following the analysis of the total system cost inefficiencies in Section 4.2, this section continues with a detailed, 15-minute resolution analysis of the power system's optimal dispatch, addressing the allocation of limited generation capacity among Energy production and the two primary Reserve products, automatic Frequency Restoration Reserve (aFRR) and manual Frequency Restoration Reserve (mFRR). This analysis moves beyond the total cost metrics of Section 4.2 to demonstrate how different operational conditions and market structures influence the commitment and output of flexible generation assets over a 24 hour period.

The allocation process is constrained by two critical factors: the physical limits of each technology, like maximum output, minimum runtime, and ramp rate limits, and the inherent opportunity cost arising from committing the same capacity to multiple energy products. The following subsections systematically break down these dynamics. To isolate the effects of demand and Variable Renewable Energy (VRE) profiles, the thesis analyzes seasonal differentiations in Section 4.3.1 and day-type ones in Section 4.3.2. The results used are primarily from the co-optimization model, which represents the most efficient, technically feasible allocation. Section 4.3.3 then introduces the core comparison, illustrating how the structural separation of markets in sequential designs leads to suboptimal resource commitment and generation schedules, which in turn explains the origins of the financial inefficiencies quantified in Section 4.2.

For clear interpretation, each generation technology in the following figures is consistently represented by the labels defined in Figure 4.2.

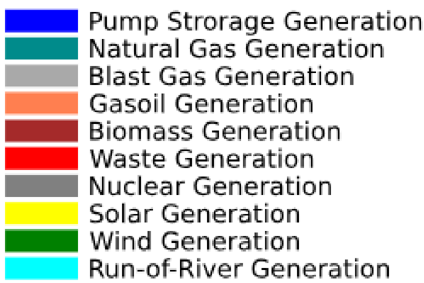

Figure 4.2: Generation Technology Labels

4.3.1 Seasonal Differentiations

This subsection analyzes the generation mix for a weekday in every season distinctively (Figure 4.3, Figure 4.4, and Figure 4.5), isolating the effect of VRE availability, total energy and reserve requirements on the dispatch schedule derived from the co-optimization model.

Energy Allocation

Figure 4.3: Seasonal Electricity Generation for a Weekday

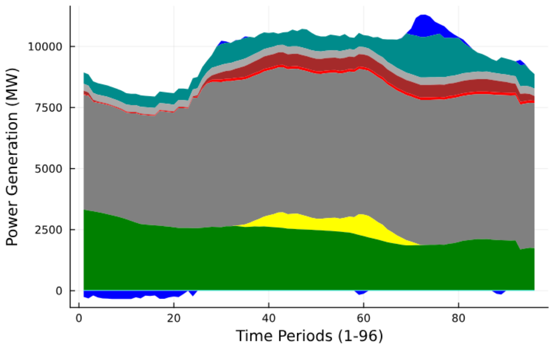

((a)) Autumn Day Electricity Generation

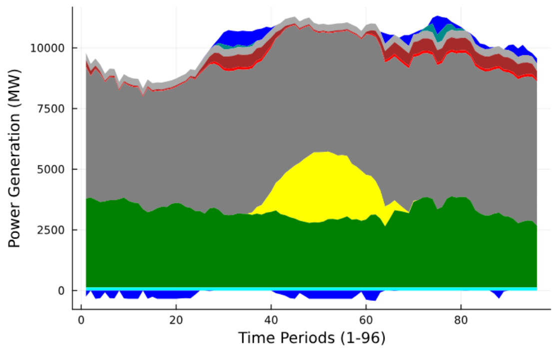

((b)) Winter Day Electricity Generation

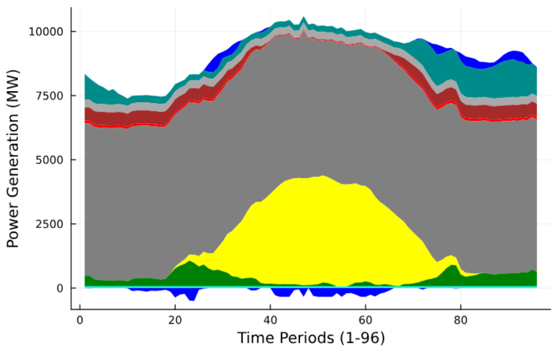

((c)) Spring Day Electricity Generation

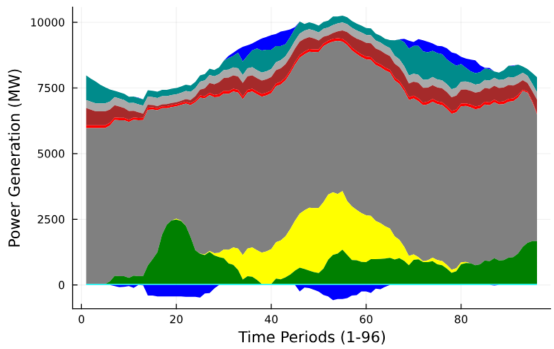

((d)) Summer Day Electricity Generation

The plots clearly reveal how the VRE profiles guide the dispatch of conventional, flexible generation. The nuclear generation, in gray, consistently provides baseload power across all seasons, reflecting its low marginal cost, high minimum capacity requirements and long minimum up/down times.

In panel (a) of Figure 4.3 autumn weekday simulation exhibits persistently high, sustained load profile, resulting in a large annual energy requirement. Wind generation (green) is stable and moderate throughout the day, providing a reliable baseload power. Solar (yellow) and run-of-river (cyan) generation on the other hand is minimal. This combination of high demand and limited VRE generation forces the majority of the high, steady net load to be covered by Nuclear (grey). Flexible thermal units meet the remaining variable demand, operating at high capacity during the day and reducing output overnight. Pumped-storage hydro (blue) is prominently used to reinforce the pronounced morning and evening peaks and store the overnight overproduction.

In panel (b) of Figure 4.3 winter weekday simulation is presented and is characterized by a high, relatively stable demand. Wind generation (green) contributes significantly and consistently throughout the day, alongside run-of-river hydro (cyan), while solar (yellow) remains low. This results in a high net load that must be covered by dispatchable units. Gasoil (teal), natural gas (dark cyan) and biomass/waste (red/dark red) operate at sustained, elevated levels to fill the gap alongside the core nuclear generation (grey) baseload. Pumped-storage hydro (blue) is deployed during the morning and evening fluctuations, while it pumps during the night when demand is low and midday when solar generations is high.

In panel (c) of Figure 4.3 spring weekday simulation is defined by high solar generation (yellow), while wind (green) and run-of-river (cyan) are virtually non-existent for the 24 hours. The strong solar input alone creates the narrowest midday net load trough of all seasons, forcing conventional generation at its minimum capacity limit. To maintain grid balance and absorb this large VRE surplus, pumped-storage hydro (blue) is forced to pump during the solar generation period. Flexible thermal generation is sharply curtailed during this time, reserved for managing the steep demand ramps in the early morning and late evening.

In panel (d) of Figure 4.3 summer weekday simulation is distinguished by unstable VREs. Solar generation (yellow) is low, run-of-river (cyan) near zero and wind (green) is wildly fluctuating, but mostly low. This results in a high degree of net load variability. The system relies heavily on the pumped-storage hydro (blue) to manage this rapid instability, scheduling it for absorbance at peak generation of VREs and frequent output adjustments during the day and evening. Except from used to quickly fill transient gaps created by the fluctuating wind it executes steep ramp-up/down with natural gas (dark cyan) to cover morning and evening demands.

aFRR Upward and Downward Allocation

Figure 4.4: Seasonal aFRR Upward and Downward Allocation for a Weekday

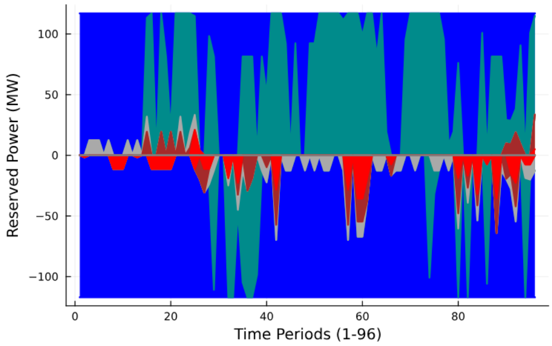

((a)) Autumn Day aFRR Allocation

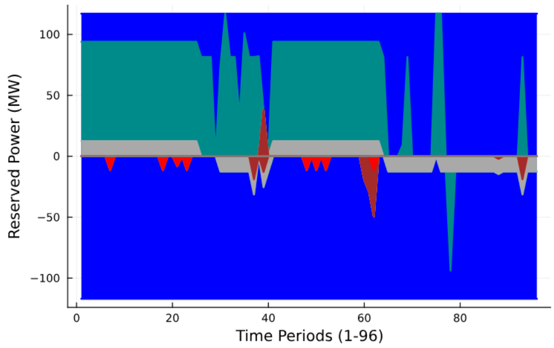

((b)) Winter Day aFRR Allocation

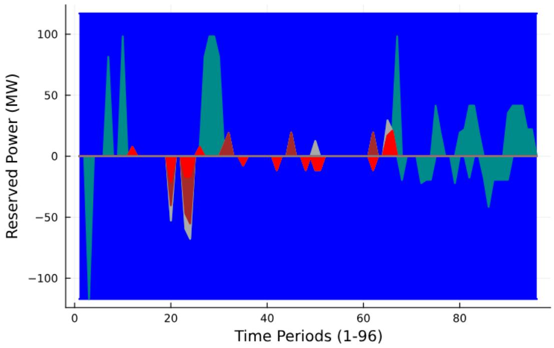

((c)) Spring Day aFRR Allocation

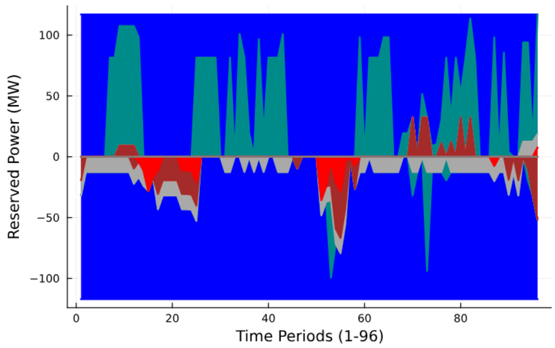

((d)) Summer Day aFRR Allocation

The aFRR, system's fastest reserve product, show its allocation is dominated by the most flexible generation pumped-storage Hydro (blue) and Natural Gas (dark cyan). In reserve plots, both upward and downward are presented jointly in the same plot, with upward in the positive region and downward in the negative.

In panels (a) and (b) of Figure 4.4, autumn and winter weekday simulation accordingly, display a balanced reliance on both pumped-storage Hydro and committed natural gas units for upward reserve. However, pumped-storage hydro provides the most of the downward reserve as it has greater capacity to absorb surplus power or reducing generation quickly.

Panel (c) of Figure 4.4 presents the spring weekday simulation, where the high solar generation that creates the narrow midday net load, necessitates large pumping storage. Consequently, pumped-storage hydro's allocation for reserve is at the highest in this season to manage the VRE surplus and associated uncertainty. The reliance on pumped-storage hydro for reserve is driven also by the need of natural gas for energy.

Panel (d) of Figure 4.4 shows the summer weekend simulation, where the unstable VRE profile, with fluctuating wind and low solar generation, causes net load with high volatility. Pumped-storage Hydro is used intensely for both upward and downward aFRR, as it can switch between generating and pumping to provide maximum rapid response capacity throughout the day, in order to face the high uncertainty.

mFRR Upward and Downward Allocation

Figure 4.5: Seasonal mFRR Upward and Downward Allocation for a Weekday

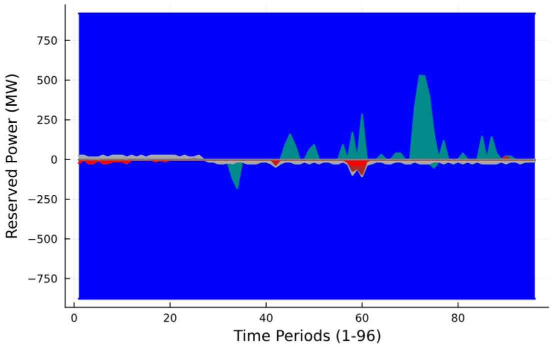

((a)) Autumn Day mFRR Allocation

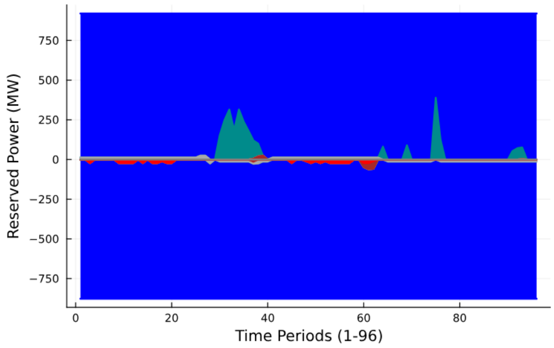

((b)) Winter Day mFRR Allocation

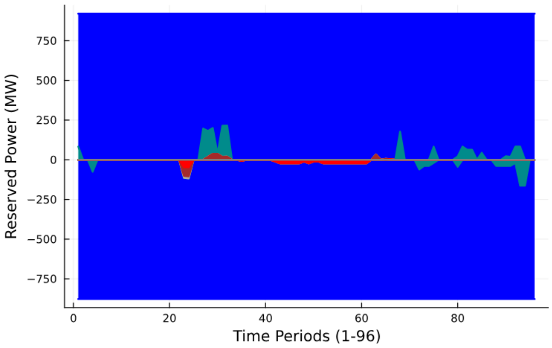

((c)) Spring Day mFRR Allocation

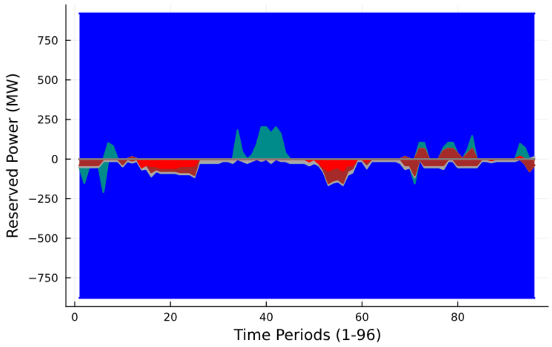

((d)) Summer Day mFRR Allocation

The allocation of mFRR, which provides a slower but with higher capacity system response, is consistently dominated by the Belgian system's most abundant flexible asset, pumped-storage hydro (blue).

The general pattern in mFRR allocation, across all seasons, is the dominant resourcing of pumped-storage hydro (blue) for both upward and downward mFRR. Its large capacity and relatively fast response (compared to conventional thermal units) make it the most economical choice for this bulk reserve product. The thermal generators are speared for energy production. Natural gas (dark cyan) and biomass/waste (red/dark red) typically fill the remaining requirements, particularly the upward reserve when pumped-storage hydro is operating near its generation or pumping limits. Additionally, in the summer, when the available water capacity for downward reserve is strained due to existing pumping schedules for energy generation, biomass/waste (red/dark red) are used for the downward mFRR mix, resources with lower cost. The consistency of pumped-storage hydro's dominance in covering mFRR, regardless of the season, highlights its structural importance as the key large-scale flexible asset in the Belgian system.

4.3.2 Day Types' Differentiations

This subsection analyzes the system dispatch with the optimal Co-optimization under demanding winter seasonal conditions, focusing on the differences in resource allocation between a Weekday (WD) when the load is higher and a Weekend Day (WE) when it gets lower. These operational differences, presented in Figure 4.9 (Energy), Figure 4.7 (aFRR), and Figure 4.8 (mFRR), are purely the result of variations in the net load profile.

Energy Allocation

Figure 4.6: Different Day Type Energy Generation in Winter

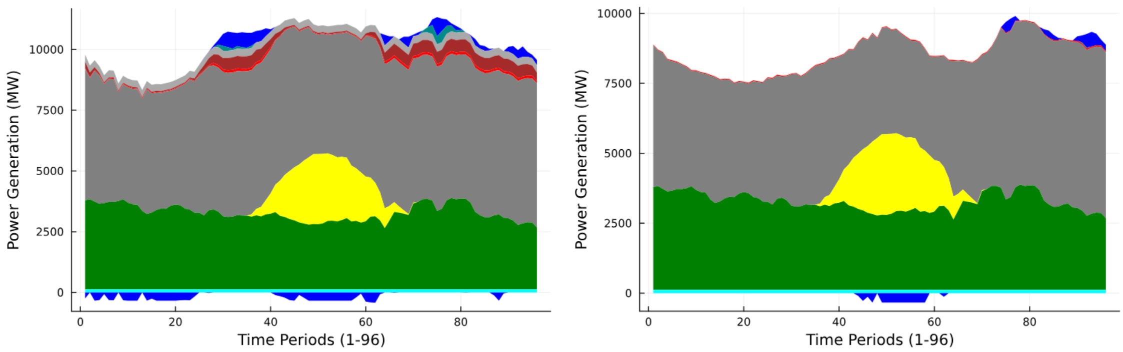

((a)) Weekday Energy Generation ((b)) Weekend Day Energy Generation

The main difference between the Weekday (4.6(a)) and the Weekend Day (4.6(b)) lies in the total load and its shape, while the VRE profile remains nearly identical, isolating the impact of human consumption patterns.

Weekday (4.6(a)) exhibits a more uniform and sustained load profile. This shape is typical of high industrial, commercial, and public service activity which runs consistently throughout the day. To satisfy this high, steady demand, thermal generation is dispatched at a higher, steady output across most of the 24 hours. Pumped-storage hydro (blue) is used minimally, primarily to ensure smooth transitions between periods and flatten out periods with increased variability.

The total load in the weekend day (4.6(b)) shows two distinct peaks in energy production, midday and evening, making its profile more variable. This pattern is explained by the closure of industrial sites and commercial businesses, which shifts demand mainly to residential consumption. Pumped-storage Hydro plays a critical, dynamic role. It pumps during the midday Solar peak to absorb energy and then switches to generating to meet the sleep evening peak that the inflexible Nuclear (gray) baseload cannot cover. Because pumped-storage Hydro successfully addresses both the storage requirement and the peak generation ramps, the other thermal units are not required to commit, so they shut down, significantly lowering the overall cost of energy production on that Winter Weekend Day.

aFRR Upward and Downward Allocation

The allocation of aFRR capacity, both upward and downward, is dominated by pumped-storage hydro commitment.

Figure 4.7: Different Day Types aFRR Allocation in Winter

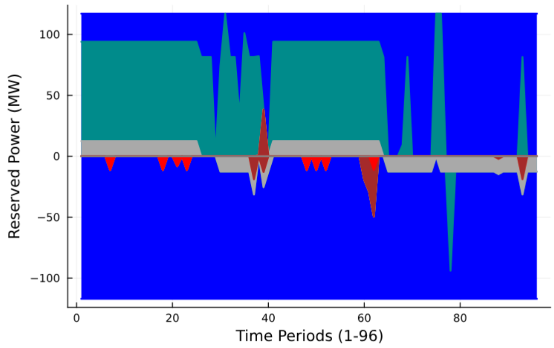

((a)) Weekday Energy Generation

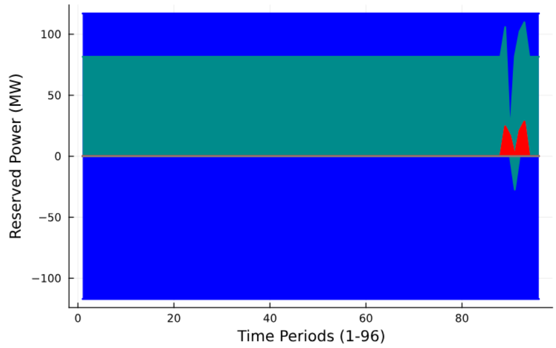

((b)) Weekend Day Energy Generation

Due to the high, sustained energy commitment of thermal units (Figure 4.6(a)), the weekday (4.7(a)) utilizes a greater mix of thermal units for aFRR, whereas in the weekend day (4.7(b)) the thermal units committed, mostly natural gas, are the ones with high ramp rates, allowing them to go from an off state to minimal capacity quickly.

Pumped-storage hydro in the weekend day is heavily dispatched to follow the tow peaks in energy demand, so it naturally becomes the primary contributor to both upward and downward aFRR, offering fast response capacity from its considerable flexibility in operations.

mFRR Upward and Downward Allocation

Figure 4.8: Different Day Types mFRR Allocation in Winter

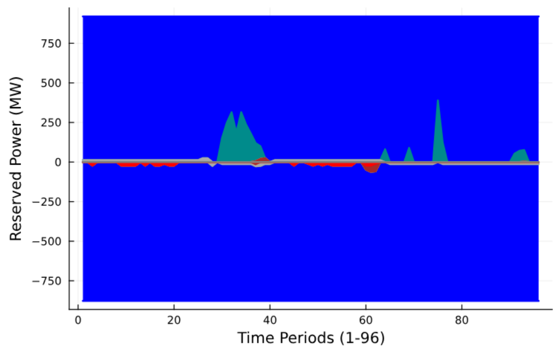

((a)) Weekday Energy Generation

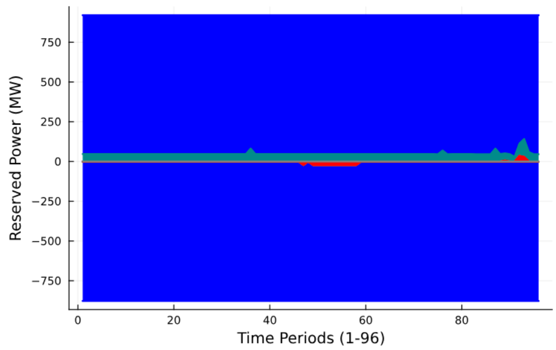

((b)) Weekend Day Energy Generation

Across both day types, pumped-storage Hydro (blue) is the overwhelming primary resource, providing virtually all of the upward and downward mFRR capacity (Figure 4.8(a) and 4.8(b)). This underscores its optimal economic role for the main system reserve. A small section mFRR is allocated from thermal technologies. Specifically on the Weekend Day, where these technologies are shut down, the amount of their commitment is minimal.

4.3.3 Methodologies' Differentiations

This subsection provides the main understanding of the thesis by comparing the optimal resource dispatch from the Co-optimization model against the suboptimal allocations of the two sequential designs, applying them on the Winter Weekday peak conditions (Figure 4.9, Figure 4.10, and Figure 4.11). The analysis reveals how the clearing process in sequential design generates the high system costs identified in Section 4.2.

Energy Allocation

Figure 4.9: Energy Generation from Different Optimization Models in a Winter Weekday

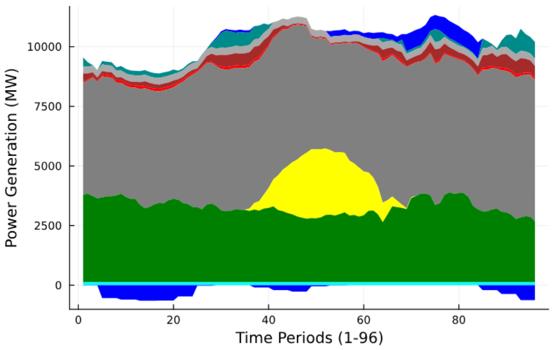

((a)) Sequential Clearing with Joint Reserves Allocation

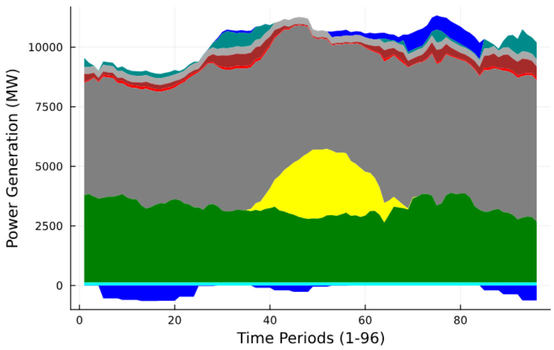

((b)) Sequential Clearing with Separate Reserves Allocation

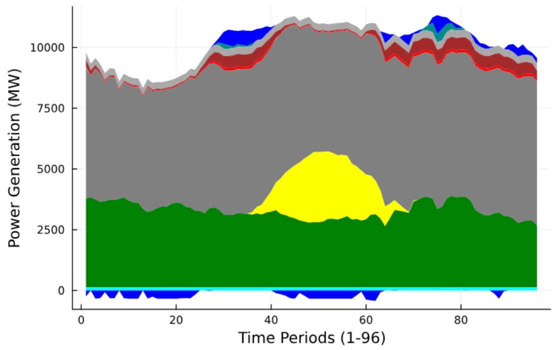

((c)) Co-optimization

The differences in energy dispatch explain the resulting cost inefficiency across the market designs. The Co-optimization model (4.9(c)) reaches the optimal solution by combining fixed costs and reserve value in one optimization, resulting in the commitment of only the most efficient thermal units needed to provide energy and ensure reserve margins. In contrast, both Sequential Clearing models (4.9(a) & 4.9(b)) show a higher dispatch of thermal units. This is due to two different reasons. First, in some periods, such as during the night, these units are committed to the prior reserve clearing stage based on an approximate energy price (λ_t), with no opportunity to adjust these decisions during subsequent energy clearing. Once committed for reserve, these costly thermal units are forced to run at their technical minimums, even when cheaper power (like pumped-storage Hydro) is available. Second, in other periods, such as early morning hours, a steep increase in load demand is observed, which is covered by expensive natural gas sources. This structural constraint, caused by the sequential approach, forces unnecessary and expensive thermal energy production, increasing the system's inefficiency.

aFRR Upward and Downward Allocation

Figure 4.10: aFRR Allocation from Different Optimization Models in a Winter Weekday

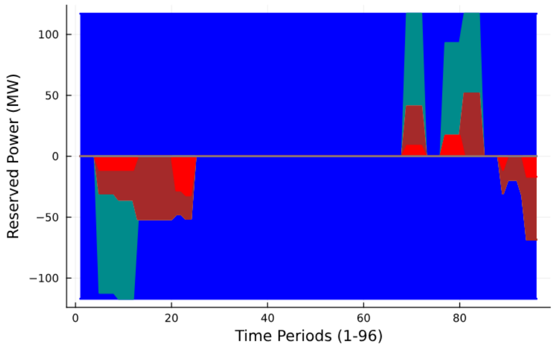

((a)) Sequential Clearing with Joint Reserves Allocation

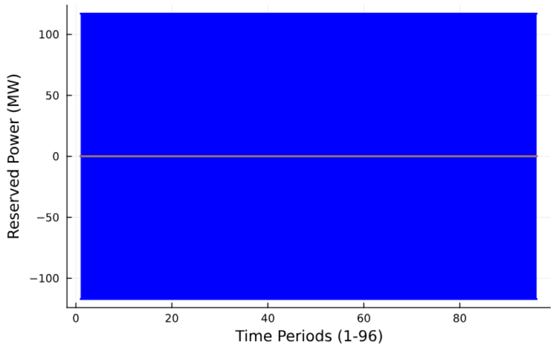

((b)) Sequential Clearing with Separate Reserves Allocation

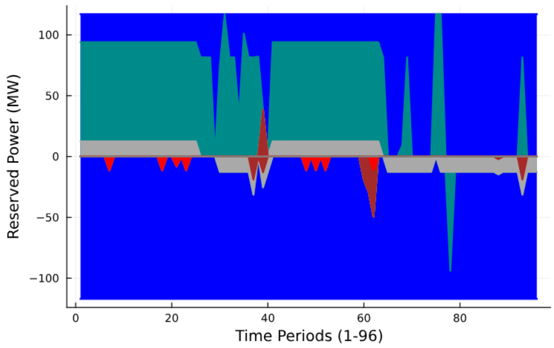

((c)) Co-optimization

The allocation of aFRR reserve capacity reveals the critical structural constraints imposed by the non-integrated market designs.

The optimal co-optimization design (4.10(c)) utilizes a dynamic and balanced mix of pumped-storage hydro (blue) and natural gas (dark cyan) for aFRR, leveraging the operating margin of the thermal fleet while using the pumped-storage hydro's flexibility.

Sequential clearing with joint reserves (4.10(a)), which clears aFRR and mFRR together, still requires the commitment of expensive units, but retains some ability to balance the two reserves.

Sequential clearing with separate reserves (4.10(b)) is the most inefficient. Because aFRR is prioritized and cleared first, the initial step inefficiently locks in pumped-storage hydro (blue) to provide all of the aFRR capacity throughout the entire day. This allocation decision severely limits pumped-storage hydro's flexibility for the other two markets of mFRR and energy, leading to inefficiency.

mFRR Upward and Downward Allocation

Figure 4.11: mFRR Allocation from Different Optimization Models in a Winter Weekday

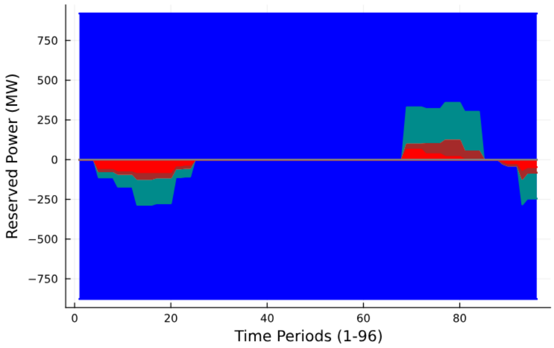

((a)) Sequential Clearing with Joint Reserves Allocation

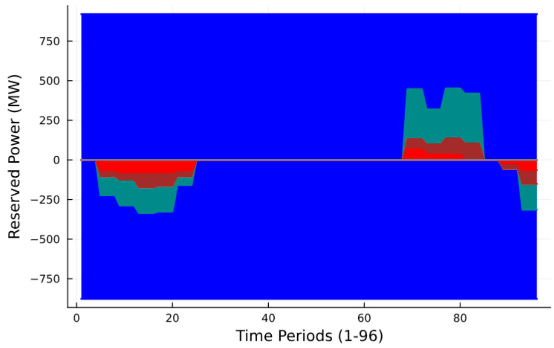

((b)) Sequential Clearing with Separate Reserves Allocation

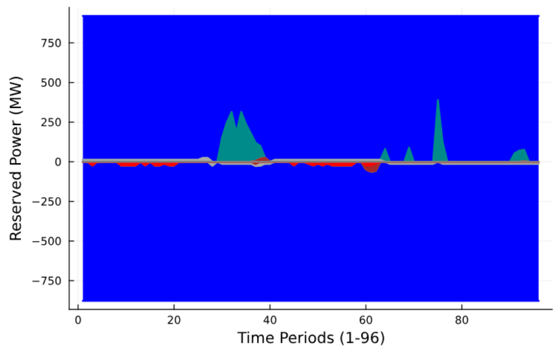

((c)) Co-optimization

The mFRR allocation is where the downstream effects of the initial reserve clearing decision become most evident, highlighting the capacity constraints imposed by prior steps.

Co-optimization (4.11(c)) allocates mFRR efficiently and minimally, primarily using pumped-storage Hydro for reserve while keeping the thermal fleet available for energy needs.

Both sequential clearing, joint and separate models (Figure 4.11(a) & 4.11(b)), allocate large blocks of thermal unit capacity for mFRR in the early and late periods of the day. Committing such a significant portion of thermal capacity to reserve, though, means that during the subsequent energy dispatch (Figure 4.9(a) & 4.9(b)), these units are required to maintain high energy output (at least their technical minimums). This locked energy production from expensive thermal units, dictated by the prior reserve decision, is the main reason that generates the substantially higher overall system costs and creates the inefficiencies noted in the sequential designs, confirming their critical financial flaw.

In summary, the co-optimization model's superior efficiency is rooted in its ability to simultaneously resolve the capacity and cost trade-offs, minimizing the overall use of expensive thermal units. The sequential models, by forcing discrete, irreversible commitments, mandate the dispatch of uneconomical thermal units, resulting in higher system operating costs.

4.4 Pumped-Storage Hydro Sensitivity

This section examines the resilience of the different market designs to flexible resource capacity limitations. In particular, it analyzes the sensitivity of cost inefficiencies by imposing a reduction in the available Pumped-Storage Hydro (PSH) generation capacity. This is achieved by applying a capacity multiplier to the original maximum generation capacity of the PSH units ($\sum_{g \in Gh} Ph_g^+$). The results are presented as percentage inefficiencies for the two sequential designs, relative to the optimal co-optimization ones at that corresponding capacity level.

The results from Table 4.6 reveal a consistent pattern: as PSH generation capacity is reduced, the inherent inefficiencies of both sequential designs grow rapidly. This sensitivity highlights the structural failure of sequential models when relying on a scarce and highly flexible resource.

In Figures 4.12 and 4.13, the winter weekend day and summer weekday scenarios have their system costs plotted against the PSH capacity multiplier to visualize the results. In both cases, the cost increase for the sequential models is exponentially greater than the corresponding cost increase for the co-optimization model, showing the disproportionate loss of efficiency.

Figure 4.12: System Cost vs. PSH Capacity Multiplier for Summer Weekday

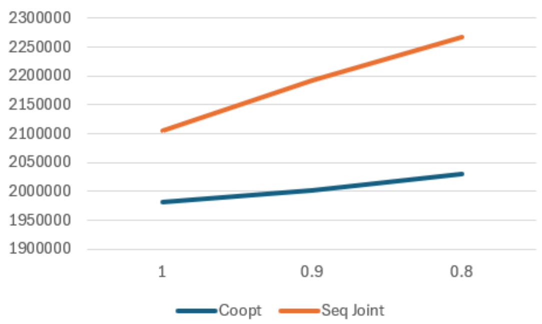

((a)) Sequential Clearing with Joint Reserves (SU-WD)

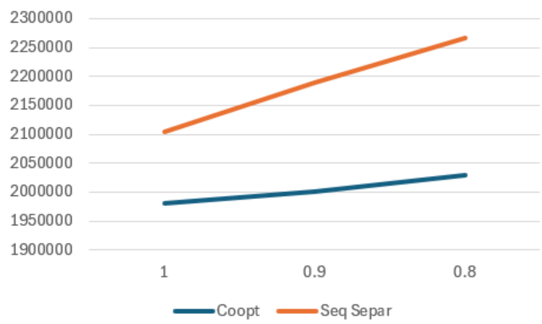

((b)) Sequential Clearing with Separate Reserves (SU-WD)

The sequential models become increasingly inefficient as their optimization process consists of several stages and forces the commitment of inefficient resources. The initial reserve clearing step must secure adequate capacity using the energy price approximation (λ_t). When PSH generation capacity is high, with multiplier equal to 1, this is achieved with minimal reliance on expensive thermal units. However, as PSH generation capacity is constrained, like when the multiplier is 0.8, the reserve

Season & Day Type	Capacity Mult.	Coopt €	Seq. J. €	Inef. %	Seq. S. €	Inef. %
AutumnWD	1	2171680	2248550	3.42	2248416	3.41
	0.9	2176453	2324832	6.38	2333654	6.74
	0.8	2198419	2415403	8.98	2413256	8.90
AutumnWE	1	1116137	1225743	8.94	1225800	8.95
	0.9	1121031	1288379	12.99	1288125	12.97
	0.8	1128876	1406546	19.74	1394965	19.07
WinterWD	1	1372060	1580779	13.20	1580777	13.20
	0.9	1389289	1641431	15.36	1641122	15.35
	0.8	1430035	1760983	18.79	1756740	18.60
WinterWE	1	828047	1045128	20.77	1045177	20.77
	0.9	832446	1107169	24.81	1103486	24.56
	0.8	837158	1206927	30.64	1206479	30.61
SpringWD	1	2029704	2219903	8.57	2220026	8.57
	0.9	2038922	2269087	10.14	2263636	9.93
	0.8	2063433	2334020	11.59	2322091	11.14
SpringWE	1	1322172	1547376	14.55	1547380	14.55
	0.9	1324196	1619887	18.25	1619673	18.24
	0.8	1336797	1680644	20.46	1680289	20.44
SummerWD	1	1981152	2104766	5.87	2104762	5.87
	0.9	2001888	2191538	8.65	2189485	8.57
	0.8	2029303	2267300	10.50	2266868	10.48
SummerWE	1	1404564	1584777	11.37	1584811	11.37
	0.9	1411446	1672456	15.61	1668947	15.43
	0.8	1439333	1736526	17.11	1736361	17.11

Table 4.6: Inefficiencies for Changing Pumped-Storage Hydro Capacity

Figure 4.13: System Cost vs. PSH Capacity Multiplier for Winter Weekend Day

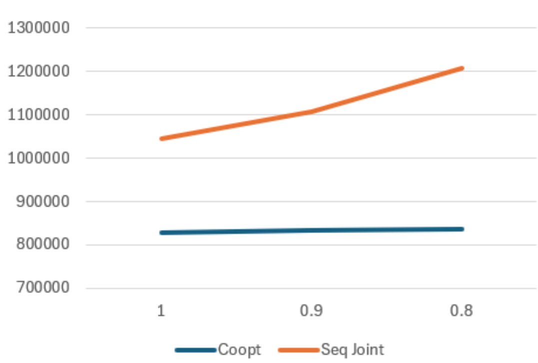

((a)) Sequential Clearing with Joint Reserves (WI-WE)

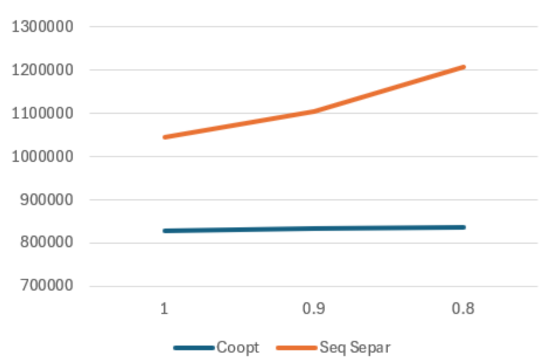

((b)) Sequential Clearing with Separate Reserves (WI-WE) clearing is forced to commit expensive thermal units to guarantee the required reserve margin. Once these high-cost units are committed, they are obliged to run at their technical minimum generation limits, even when economic conditions in the later energy clearing stage do not require it. This commitment of expensive, inflexible capacity is the mechanism that drives the sharp increase in inefficiency. The highest inefficiency, exceeding 50% (panels (a) and (b) in Figure 4.13), is observed in the winter weekend day scenario, where load variability and low PSH capacity exacerbate this commitment risk.

This vulnerability eventually renders the sequential methodology unworkable under extreme scarcity. When the PSH generation capacity multiplier is reduced below 0.8, for example to 0.6, the sequential model becomes infeasible, indicating that the rigid, prioritized allocation of reserve first locks up essential resources, preventing the subsequent energy allocations from securing the total required capacity. The co-optimization model, by evaluating all constraints simultaneously, successfully finds a feasible, more financially efficient, solution even under these challenging resource limitations.

Chapter 5

Conclusion

This thesis systematically analyzed the efficiency of different market-clearing mechanisms for energy and reserves, aimed to compare co-optimization and sequential clearing approaches. Based on a comprehensive mathematical framework implemented and solved in Julia using the Gurobi solver, three distinct models were formulated and assessed: a co-optimization model, a sequential model with joint reserve allocation, and a sequential model with separate clearing of reserve types (aFRR followed by mFRR).

The results reveal the advantage of co-optimization clearing, that consistently delivers more efficient outcomes, as it simultaneously accounts for the interdependencies between energy and reserves. Sequential designs, in contrast, introduce structural inefficiencies because of their multistage clearing. These inefficiencies arise mainly from the misallocation of fixed costs and the failure to fully capture how energy generation and reserve services are connected.

In the Belgian case study, the inefficiency of the sequential clearing models resulted in an annual cost deviation of up to 12.72%, for the sequential with separate reserve clearing model, relative to the optimal co-optimization, which translates into 82.6 million €. Separate clearing of reserves produces an additional 1.01% inefficiency, added to the already large financial loss. This wastage is driven by the fact that the sequential approach forces the unnecessary commitment of expensive thermal units to run at their technical minima, even when more efficient power sources are available during the subsequent energy dispatch phase, such as from pumped-storage hydro (PSH). The analysis of resource allocation confirms this behavior, revealing that PSH is the key flexible resource whose optimal deployment is undermined by sequential clearing. The co-optimization model makes full use of PSH's operational margin for both energy and reserve, whereas the sequential prioritization of the faster reserve (aFRR) inefficiently locks in PSH capacity, forcing a costly over-reliance on gas-fired generation in later stages.

Furthermore, the PSH sensitivity analysis highlighted a critical weakness of the sequential market design. As the PSH generation capacity was reduced, the inefficiency of both sequential models escalated sharply, demonstrating their lack of resilience under resource scarcity. When PSH capacity was constrained below 0.65 of its nominal value, a significant change observed was that the sequential with separate reserve clearing model became mathematically infeasible. This proved that its inflexible, subsequent clearing process fails to secure the necessary reserves when flexible resources are limited.

Beyond the analytical results, the thesis also demonstrates the practicality of coding such formulations in Julia. The framework developed here is modular and can be easily extended to include additional complexities such as network constraints, fluctuating renewable energy profiles, or reserve capacity exchange between countries. As such, it provides a valuable computational tool for future studies.

In summary, the results support the case for adopting co-optimization of energy and reserves within European electricity markets. By reducing total system costs and improving resource allocation, co-optimization represents a significant step toward achieving both economic efficiency and reliability in the operation of increasingly renewable dominated power systems. Future research could build on this work by applying the analysis to broader regions, investigating the effects of transmission limitations, or incorporating strategic bidding behavior to better capture market dynamics.

Bibliography

[1] Amit Mathrani, "The rise of electric vehicles in the US: Impact on the electricity grid - Rabobank," Rabobank, 2024. Available:
https://www.rabobank.com/knowledge/d011456343-the-rise-of-electric-vehicles-in-the-us-impact-on-the-electricity-grid

[2] M. Ventosa, Á. Baíllo, A. Ramos, and M. Rivier, "Electricity market modeling trends," Energy Policy, vol. 33, no. 7, pp. 897–913, May 2005, doi: 10.1016/j.enpol.2003.10.013. Available:
https://repositorio.inesctec.pt/server/api/core/bitstreams/0f07adc1-2e8a-4bf8-a6c9-d24116394457/content

[3] M. Ventosa, Á. Baíllo, A. Ramos, and M. Rivier, "Electricity market modeling trends," Energy Policy, vol. 33, no. 7, pp. 897–913, May 2005, doi: 10.1016/j.enpol.2003.10.013. Available:
https://www.sciencedirect.com/science/article/abs/pii/S0142061519308373

[4] R. Carmona and M. Coulon, "A survey of commodity markets and structural models for electricity prices," Princeton University, Princeton, NJ, USA, 2014. Available: https://onlinelibrary.wiley.com/doi/full/10.1002/for.2693

[5] P. González, J. Villar, C. A. Díaz, and F. A. Campos, "Joint energy and reserve markets: Current implementations and modeling trends," Electric Power Systems Research, vol. 109, pp. 101–111, Feb. 2014, doi: 10.1016/j.epsr.2013.12.010. Available:
https://www.sciencedirect.com/science/article/abs/pii/S0301421519300564

[6] E. Delarue, W. D'haeseleer, and P. Duerinck, "Coupling between energy and reserve markets in European electricity systems," Electric Power Systems Research, vol. 189, pp. 106–119, Jul. 2020, doi: 10.1016/j.epsr.2020.106599. Available:
https://www.sciencedirect.com/science/article/abs/pii/S0378779620303412

[7] G. Doorman and van, "An analysis of design options for markets for cross-border balancing of electricity," vol. 27, pp. 39–48, Dec. 2013, doi:
https://doi.org/10.1016/j.jup.2013.09.004.

[8] E. G. Read, "Co-Optimization of Energy and Ancillary Service Markets," Energy Systems, pp. 307–327, 2010, doi: https://doi.org/10.1007/978-3-642-02493-1_13.

[9] R. Wilson, "Architecture of Power Markets," Econometrica, vol. 70, no. 4, pp. 1299–1340, 2002, doi: https://doi.org/10.2307/3082000.

[10] V. Ahlqvist, P. Holmberg, and T. Tangerås, "Central- versus Self-Dispatch in Electricity Markets," SSRN Electronic Journal, Jan. 2018, doi:
https://doi.org/10.2139/ssrn.3302569.

[11] European Commission, "Commission Regulation (EU) 2017/1485 of 2 August 2017 establishing a guideline on electricity transmission system operation," Official Journal of the European Union, vol. L 220, pp. 1–120, Aug. 25, 2017.

[12] S. Borenstein, J. B. Bushnell, and F. A. Wolak, "Measuring Market Inefficiencies in California's Restructured Wholesale Electricity Market," American Economic Review, vol. 92, no. 5, pp. 1376–1405, Nov. 2002, doi: https://doi.org/10.1257/000282802762024557.

[13] A. Riascos, M. Bernal, L. de Castro, and S. Oren, "Transition to Centralized Unit Commitment: An Econometric Analysis of Colombia's Experience," The Energy Journal, vol. 37, no. 3, pp. 271–292, Jul. 2016, doi: https://doi.org/10.5547/01956574.37.3.aria.

[14] A. Papavasiliou and Y. Smeers, "Remuneration of Flexibility using Operating Reserve Demand Curves: A Case Study of Belgium," The Energy Journal, vol. 38, no. 01, Sep. 2017, doi: https://doi.org/10.5547/01956574.38.6.apap.

[15] L. M. Silva Rodriguez, Electricity Market Design Under Uncertainty: Supporting the Integration of Large-Scale Renewable Energy Sources, Ph.D. dissertation, Copernicus Institute of Sustainable Development, Utrecht Univ., Utrecht, The Netherlands, 2024. doi: 10.33540/2581.

[16] K. De Vos, N. Stevens, O. Devolder, A. Papavasiliou, B. Hebb, and J. Matthys-Donnadieu, "Dynamic dimensioning approach for operating reserves: Proof of concept in Belgium," Energy Policy, vol. 124, pp. 272–285, Jan. 2019, doi: https://doi.org/10.1016/j.enpol.2018.09.031.

[17] G. G. Dranka, P. Ferreira, and A. I. F. Vaz, "A review of co-optimization approaches for operational and planning problems in the energy sector," Applied Energy, vol. 304, p. 117703, Dec. 2021, doi: https://doi.org/10.1016/j.apenergy.2021.117703.

[18] P. R. Milgrom, Putting Auction Theory to Work, Cambridge, U.K.: Cambridge Univ. Press, 2004.

[19] A. Ehrenmann and Y. Smeers, "Inefficiencies in European Congestion Management Proposals," SSRN Electronic Journal, 2004, doi: https://doi.org/10.2139/ssrn.746506.

[20] Deeban Chakravarthi, "Power System Economics Designing Markets for Electricity," Scribd, 2018. https://www.scribd.com/doc/66440034/Power-System-Economics-Designing-Markets-for-Electricity.

[21] Alberta Electric System Operator, "Refinement to Comparison between sequential selection and co-optimized markets," Alberta Electric System Operator, Alberta, Canada, 2018.

[22] V. Dawar, B. C. Lesieutre, and T. P. Bohn, “Effects of co-optimization of energy and reserves on prices,” 2011 North American Power Symposium, pp. 1–6, Aug. 2011, doi: https://doi.org/10.1109/naps.2011.6025168.

[23] Yonas Gebrekiros, G. Doorman, S. Jaehnert, and H. Farahmand, “Bidding in the Frequency Restoration Reserves (FRR) market for a Hydropower Unit,” Innovative Smart Grid Technologies Europe (ISGT EUROPE), 2013 4th IEEE/ PES, pp. 1–5, Oct. 2013, doi:

https://doi.org/10.1109/ISGTEurope.2013.6695362.

[24] “Benefits of cross-border reserve procurement based on pre-allocation of transmission capacity - SINTEF,” SINTEF, 2025.

https://www.sintef.no/publikasjoner/publikasjon/1038505/ (accessed Oct. 12, 2025).

[25] S. Just and C. Weber, “Pricing of reserves: Valuing system reserve capacity against spot prices in electricity markets,” Energy Economics, vol. 30, no. 6, pp. 3198–3221, Nov. 2008, doi: https://doi.org/10.1016/j.eneco.2008.05.004.

[26] “Market-Clearing Electricity Prices and Energy Uplift — Harvard Electricity Policy Group,” Harvard.edu, 2025.

https://hepg.hks.harvard.edu/publications/market-clearing-electricity-prices-and-energy-uplift (accessed Oct. 12, 2025).

[27] M. Backer, D. Keles, and E. Kraft, “The economic impacts of integrating European balancing markets: The case of the newly installed aFRR energy market-coupling platform PICASSO,” Energy Economics, vol. 128, p. 107124, Dec. 2023, doi: https://doi.org/10.1016/j.eneco.2023.107124.

[28] A. Papavasiliou, “Multi-Area Reserve Dimensioning Using Chance-Constrained Optimization,” IEEE Transactions on Power Systems, vol. 36, no. 3, pp. 2768–2778, May 2021, doi: 10.1109/TPWRS.2021.3054825. Available:

https://ieeexplore.ieee.org/stamp/stamp.jsp?arnumber=9640553

[29] A. Papavasiliou, ”Scarcity Pricing and the Missing European Market for Real-Time Reserve Capacity,” Energy Policy, vol. 144, p. 111648, 2020, doi: 10.1016/j.enpol.2020.111648. Available:

https://dial.uclouvain.be/pr/boreal/object/boreal:259554/datastream/PDF

[30] A. Papavasiliou, Y. Smeers, and G. de Maere d’Aertrycke, “Market Design Considerations for Scarcity Pricing: A Stochastic Equilibrium Framework,” Energy Economics, vol. 104, p. 105633, 2021, doi: 10.1016/j.eneco.2021.105633. Available: https://ap-rg.eu/wp-content/uploads/2020/10/J26.pdf

[31] A. Papavasiliou and D. Ávila, ”Welfare Benefits of Co-Optimising Energy and Reserves,” European Union Agency for the Cooperation of Energy Regulators, ACER, Ljubljana, Slovenia, 2024.

[32] A. Papavasiliou, Optimization Models in Electricity Markets. Cambridge University Press, 2024.